

# Vacuum Arc Commutator for Resistive Fault Current Limiter

---

EL-1187  
Research Project 993-2

Final Report, September 1979

Prepared by

GOULD-BROWN BOVERI  
100 County Line Road  
Colmar, Pennsylvania 18915

Principal Investigators  
Rolf Dethlefsen  
J. Mylius

Prepared for

Electric Power Research Institute  
3412 Hillview Avenue  
Palo Alto, California 94304

EPRI Project Managers  
Richard E. Kennon  
Joseph W. Porter  
Ivars Vancers  
Electrical Systems Division

## **DISCLAIMER**

**Portions of this document may be illegible in electronic image products. Images are produced from the best available original document.**

#### ORDERING INFORMATION

Requests for copies of this report should be directed to Research Reports Center (RRC), Box 50490, Palo Alto, CA 94303, (415) 961-9043. There is no charge for reports requested by EPRI member utilities and affiliates, contributing nonmembers, U.S. utility associations, U.S. government agencies (federal, state, and local), media, and foreign organizations with which EPRI has an information exchange agreement. On request, RRC will send a catalog of EPRI reports.

~~Gould-Brown Boveri Colmar, Pennsylvania~~

EPRI authorizes the reproduction and distribution of all or any portion of this report and the preparation of any derivative work based on this report, in each case on the condition that any such reproduction, distribution, and preparation shall acknowledge this report and EPRI as the source.

#### NOTICE

This report was prepared by the organization(s) named below as an account of work sponsored by the Electric Power Research Institute, Inc. (EPRI). Neither EPRI, members of EPRI, the organization(s) named below, nor any person acting on their behalf: (a) makes any warranty or representation, express or implied, with respect to the accuracy, completeness, or usefulness of the information contained in this report, or that the use of any information, apparatus, method, or process disclosed in this report may not infringe privately owned rights; or (b) assumes any liabilities with respect to the use of, or for damages resulting from the use of, any information, apparatus, method, or process disclosed in this report.

Prepared by  
Gould-Brown Boveri  
Colmar, Pennsylvania

## ABSTRACT

A triggered vacuum arc commutating switch, based on magnetic modulation has been evaluated for application to a resistive fault current limiter at transmission voltages.

A self-contained turn-on, turn-off switch has been demonstrated for the multi-MW power level. Up to 9 kA have been interrupted. Transient recovery voltages ranged up to 20 kV.

Parallel shunt capacitance increases the interruption ability, particularly at higher source voltages.



## EPRI PERSPECTIVE

### PROJECT DESCRIPTION

Limiting the magnitude of short circuit current that can flow during a fault would enable utilities to indefinitely postpone replacement of existing equipment that can no longer handle increased fault current due to system growth. It would also permit reduction of fault current withstand requirements of new equipment. This is the final report on the experimental phase of this project by Gould Inc., which investigated a triggered, vacuum-arc commutating switch for use as a component in a resistive fault current limiter (FCL) for application at transmission voltages. It builds upon the work of EPRI Research Project (RP) 476-1 and will be supplemented in the near future with a separate report (RP993-1) that describes the companion theoretical and diagnostic work performed by the State University of New York at Buffalo.

### PROJECT OBJECTIVES

The objectives of this one-year project were to investigate and optimize the operation of a magnetically-modulated, vacuum-arc, fault-commutating device and to determine the feasibility of using this fast-acting switch in a particular application. In this application it would be triggered into conduction to divert the fault current from a fast-acting parallel bypass switch. After a short period of time to allow the bypass switch to deionize, it would then be magnetically switched off to insert a current limiting resistor.

### PROJECT RESULTS

Reliable turn-on was demonstrated. Reliable interruption in the range from 5 to 6.5kA was obtained with maximum values up to 9kA. Transient recovery voltage capability was demonstrated up to 20kV. With the performance levels currently foreseen, other methods being investigated in related studies appear to be less

complex for application at transmission voltages. The concept could prove useful as a high power switching device where its inherent high speed would permit very high, repetitive switching rates.

Joe Porter, Project Manager  
Electrical Systems Division

## ACKNOWLEDGMENTS

The research project described in this report was sponsored by the Electrical Systems Division of the Electric Power Research Institute. The authors appreciate the guidance and support given by the Program Manager, Dr. Narain Hingorani and by the three successive EPRI Project Managers, Joseph W. Porter, Richard E. Kennon and Ivars Vancers. Connection with the requirements of practical application for fault current limiters was provided by the Industry Advisors whose judgement shaped this project.

Olin Compton, Virginia Electric Power Company

Leo Edwards, Tennessee Valley Authority

Lu Kolarik, Philadelphia Electric Company

Leonard Long, Duke Power Company

A stimulating cooperation existed with the State University of New York at Buffalo, namely with Dr. A. S. Gilmour and Dr. Richard Dollinger.

The contributions of the following personnel from Gould-Brown Boveri are gratefully acknowledged: Tom Dodds, Peter Kroon, Don Weston of the R&D Division; Norm Oswalt, Joe DeSalvo and Dave Moreno who provided skillful laboratory work and Jane Eisaman who typed the manuscript. Editorial assistance was provided by John Marks of EPRI.



## CONTENTS

<u>Section</u>	<u>Page</u>
1 INTRODUCTION	1-1
2 EXPERIMENTS	2-1
Apparatus	2-1
Vacuum System and Physical Set-Up	2-1
Capacitor Bank Power Supply	2-3
Magnetic Control Field	2-4
Triggering	2-5
Measurements	2-8
Parametric Studies	2-9
Discharge Geometry	2-9
Residual Vacuum Pressure	2-12
Cathode Materials	2-14
Potential Distribution	2-17
Microwave Measurements	2-20
Effect of Magnetic Field	2-21
Vacuum Arc Impedance	2-25
Circuit Interruption Tests	2-29
Design Options	2-36
Testing in the 60 Hz Laboratory	2-40
Theory of Commutation	2-43
3 DISCUSSION	3-1
Vacuum Arc Physics	3-1
Feasibility of Application	3-3
Recommendation for Further Pursuit	3-5
References	3-6

<u>Section</u>		<u>Page</u>
APPENDIX A	BACKGROUND OF THE MAGNETICALLY MODULATED VACUUM ARC	A-1
APPENDIX B	TRIGGER OPTIONS	B-1
APPENDIX C	LITERATURE REVIEW	C-1

## ILLUSTRATIONS

<u>Figure</u>	<u>Page</u>
1 State of the Art Fault Current Limiter	1-1
2 Fault Current Limiter with Vacuum Arc Commutator	1-3
3 Test Set-Up	2-2
4 Photo of Test Set-Up	2-2
5 Switched Off Vacuum Arc	2-3
6 Magnetic Field Pulse	2-5
7 Earlier Trigger Arrangement	2-6
8 Graphite Trigger Electrode	2-7
9 Diagram of Trigger Circuit	2-7
10 Geometry with Indented Anode	2-11
11 Clean Up Discharges	2-12
12 Sealed Test Device	2-13
13 Test Device for Evaluation of Cathode Materials	2-15
14 Test Device and Floating Plasma Potentials	2-18
15 Anode Voltage with Magnetic Field Applied	2-19
16 Floating Potential at Top Plate	2-19
17 Oscillations Caused by Magnetic Field	2-21
18 Elevation of Arc Voltage	2-23
19 Arc Impedance as Function of Magnetic Field Strength	2-24
20 Arc Impedance as Function of Magnetic Field Strength	2-25
21 Arc Impedance as Function of Current	2-26
22 Arc Impedance as Function of Current	2-28
23 Interruption Ability as Function of Parallel Capacitance	2-29
24 Switched Off Vacuum Arc, No Parallel Capacitance	2-31
25 Switched Off Vacuum Arc with Parallel Capacitor	2-32
26 Interruption Ability as Function of Magnetic Field Strength	2-33
27 Interruption Ability as Function of Anode Area	2-34
28 Alternate Trigger Arrangement	2-37
29 Alternate Switching Circuit	2-38

<u>Figure</u>	<u>Page</u>
30      Diagram for 60 Hz Power Test	2-40
31      Test Oscillogram of Power Test	2-41
32      Summary of Power Tests	2-42
33      Switched Off Vacuum Arc	2-44
34      Unsuccessful Vacuum Arc Switch Off	2-47

## SUMMARY

The project goals are:

- In cooperation with the State University of New York at Buffalo (SUNY) investigate and optimize the operation of a vacuum arc commutating switch.
- Determine the feasibility of using this fast acting switch in a particular application of a resistive fault current limiter system with the following requirements:

Interruption Current 9 kA  
Recovery Voltage 60 kV Peak

The experiments were performed with typical vacuum interrupter hardware in order to apply realistic constraints.

The interruption level was raised from 800 A to a maximum value of 9,000 A. Consistent reliable interruption was attained in the 5 to 6.5 kA range.

Recovery voltages up to 20 kV were available from the test circuit. The transient recovery voltage capability of the device appears to be above 20 kV.

The design parameters were optimized with the following results:

The cathode is a metallic cylinder with internal graphite trigger electrode.

The ring-shaped anode, surrounding the cathode is made a part of the vacuum envelope wall. This design eliminates the need for troublesome current feed-throughs.

The magnetic control field is generated by a current pulse in a winding on the outside of the anode.

Commutation duty requires an arcing time up to about 1 msec. The thermal capacity of the anode does not represent a limitation in this application.

The cathode must be a vacuum refined metal with low gas content, such as cobalt, copper, titanium, aluminum, molybdenum, etc.

Increased interruption ability is attained with larger anode area and increased magnetic field strength.

Also parallel capacitance increases the interruption ability. Interruption without applied shunt capacitance can be explained by elementary theory of DC switching in an inductive circuit. The magnetically elevated arc voltage decreases the circuit current as long as its value exceeds the supply voltage. Circuit interruption occurs when the current-chop level is reached. Switching without parallel capacitance will therefore be limited to circuits with rather low supply voltage in the range of several kV.

Application of the magnetic field changes the volt-ampere characteristic of the vacuum arc from essentially positive to negative. The negative characteristic together with circuit inductance and shunt capacitance allows for self-sustained oscillation at the natural frequency of the R-L-C circuit formed by the arrangement of the vacuum device and shunt capacitance. These oscillations drive the current rapidly toward zero. Again, circuit interruption occurs at the current-chop level which is a characteristic of the cathode material.

Laboratory interruption tests were performed on an inductive circuit with power derived from a charged capacitor bank. Results were confirmed with about 250 test operations on a 60 Hz power test circuit.

A correlation of experimental observation and theory available from the literature indicates that the source of the high arc voltage generated by the magnetically modulated vacuum arc is an electron space charge layer in front of the anode.

## Section 1

### INTRODUCTION

The successful implementation of fault-current limiters into electric utility systems depends on the development of an effective commutation device for the insertion of a current limiting impedance. The essential requirement of the

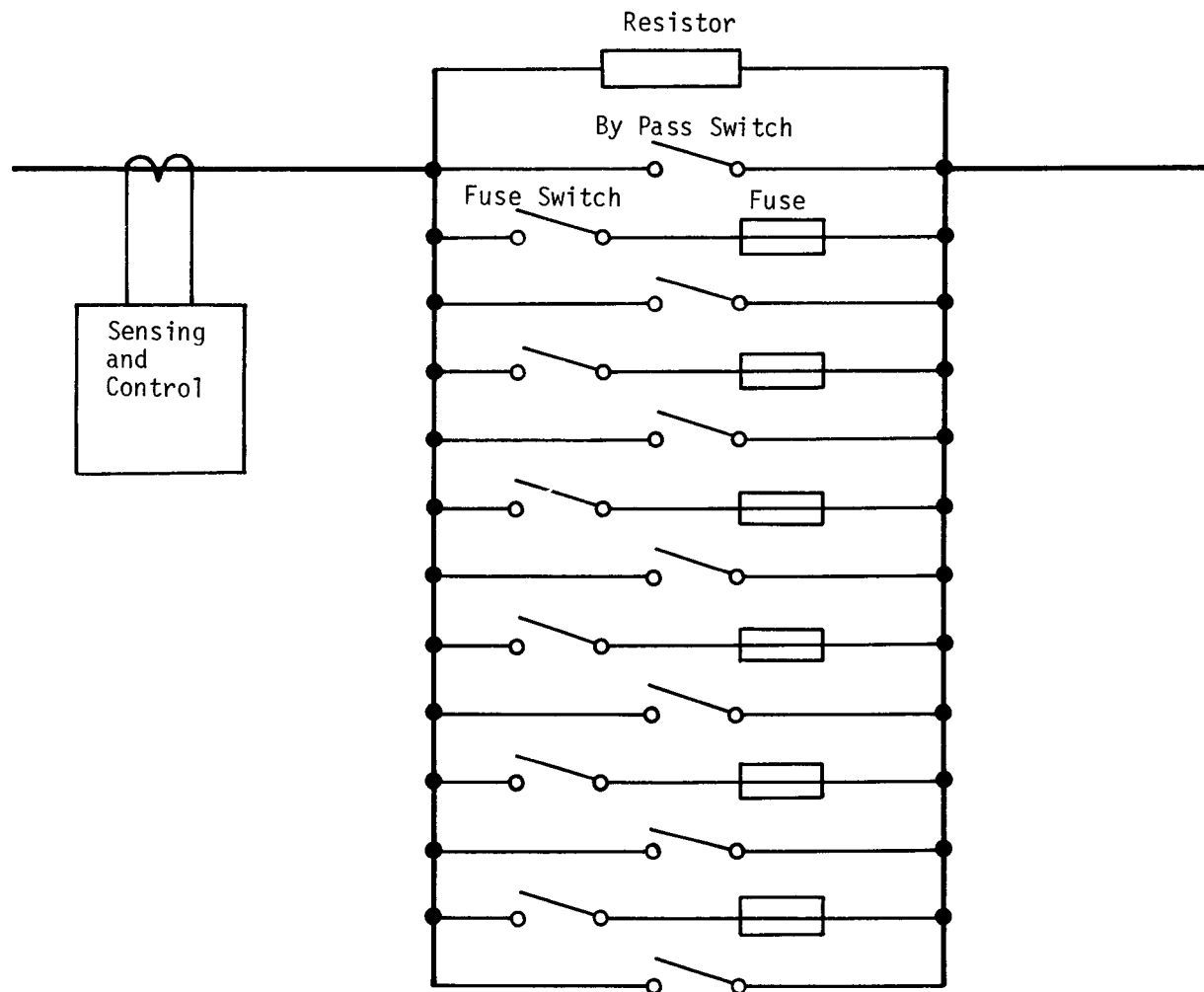


Figure 1. State of the Art Fault Current Limiter which has been demonstrated at 72.5 kV. Current Commutation is achieved with the aid of fuses.

commutation device is to generate high arc voltages very fast. Electric arcs in sand, oil or gases have been considered as switching medium for this application.

Under EPRI Contract RP 281, a fault current limiter is being developed which is described in Figure 1.

Under normal conditions one bypass switch is closed, carrying the normal load current with virtually no loss. When a fault occurs, the sensor determines the existence of the fault in 0.5 to 4 ms, depending on the fault current level and the offset. The sensor then simultaneously signals the chemically actuated bypass switch to open and its corresponding fuse switch to close. The arc voltage developed by the bypass switch commutes the current to the fuse which then melts and develops a high arc voltage to commutate current into the resistor, and limit the first loop peak current. During the first loop the current is shared by the fuse and the resistor. The fuse clears at the first current zero, and thereafter the resistor is fully inserted. The bypass switch must recover its dielectric capability during the fuse melting time. When the fault is cleared, the next bypass switch is closed, returning the FCL to its normal current-carrying state ready to operate the next fuse/switch pair for a subsequent fault.

The fault current limiter has the highest demand for reliable, consistently reproducible performance of any device on a power system. A reduction in the number of switching elements is highly desirable for increased reliability. The use of single shot fuses by necessity calls for repeater action.

The present project aims at replacing the commutation fuses and associated insertion switches with a re-usable commutating switch which utilizes magnetically modulated vacuum arcs.

A conceptual system based on the vacuum commutator is shown in Figure 2.

The current limiting resistor and the control are similar to the ones in Figure 1. A bypass switch is required for this particular application which can operate repeatedly and generate 500 V arc voltage within 1 msec after tripping, while carrying 2 kA in the closed state and recovering to about 60 kV peak voltage.

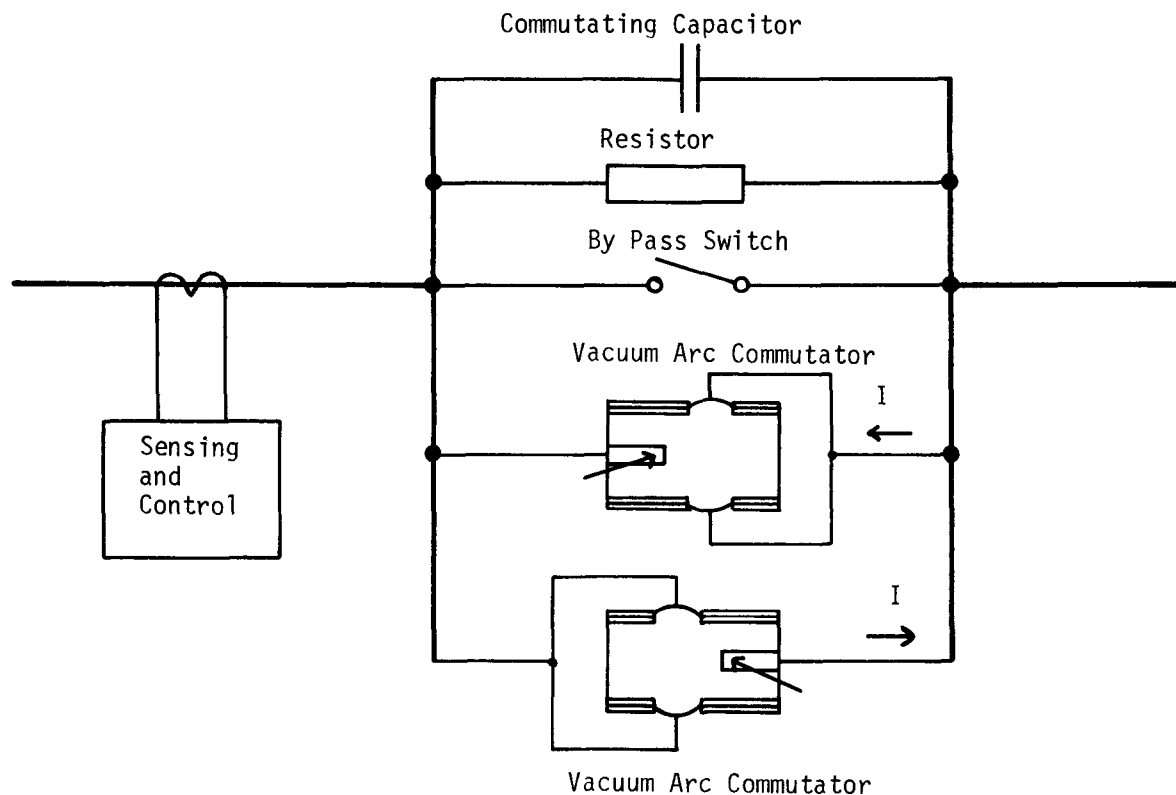


Figure 2. Fault Current Limiter with Vacuum Arc Commutator for Multiple Operations.

Two vacuum arc commutators are required for AC because these devices are polarity dependent.

The triggered vacuum device must be able to start conduction on 500 V which is the level of arc voltage generated by the bypass switch.

The resulting vacuum arc voltage must initially be low in order to allow fast current commutation. A magnetic control field is applied to the vacuum device, after all current has commutated into it and after the bypass switch has recovered. The magnetic field raises the vacuum arc voltage and commutes the current into the fault current limiting resistor. An optional commutating capacitor aids in successful current transfer from the vacuum device to the resistor.

It would be desirable to incorporate the bypass switch contacts into the vacuum device, requiring mechanically moving contacts. This entails a restriction on the possible electrode geometries and is therefore not contained in the scope of this project.

The work is done in cooperation with A. S. Gilmour and R. Dollinger of the State University of New York at Buffalo, the originator of this concept.<sup>(1)</sup> The primary goal is to determine the practical feasibility of using vacuum arc commutators for fault current limitation at transmission voltage levels. Experimentation is therefore conducted with standard vacuum interrupter hardware as opposed to larger laboratory-type bell jar vacuum systems.

Design goals were selected from a fault current limiter application at Southern California Edison which is presently pursued under EPRI Project RP-281:

Trigger Voltage	= 500 V
Current Carrying Ability	= $10^8 A^2 \cdot 10^{-3}$ sec
Interruption Current	= 9 kA
Recovery Voltage	= 60 kV peak

A. S. Gilmour originally demonstrated a switching ability of 800A at 25 kV for magnetically modulated vacuum arcs.<sup>(1), (2)</sup> In later work under EPRI, Contract 476-1, A. S. Gilmour concentrated on the steady generation of high arc voltages in vacuum arcs (self limited mode). He demonstrated that several kV of arc voltage can be generated at currents up to 10 kA.

The present effort at Gould Inc. started in Nov. '75 with a 4-month study funded by EPRI under Project RP 281-2. The Gilmour scheme of magnetic modulation of vacuum arcs was confirmed with experiments in realistically sized vacuum interrupter hardware instead of large laboratory type bell jar vacuum systems as used by Gilmour. The initial phase achieved a switching ability of 800A at 3.6 kV. Further work proceeded with Gould funding. It was realized that an anode placed inside the vacuum envelope as in Ref. 1 was leading to problems due to current attachment at the feedthrough areas. Accordingly, all further tests were performed with an anode which constitutes a part of the vacuum envelope. This eliminates the need for current feedthroughs to the anode. EPRI funding resumed in Jan. '78. This report covers results obtained during 1978.

## Section 2

### EXPERIMENTS

#### APPARATUS

Testing was conducted in a dedicated laboratory set-up with a capacitor bank as power source.

Comparison tests were also performed on a 60 Hz power test laboratory circuit.

#### Vacuum System and Physical Set-Up

Most of the experiments used demountable vacuum envelopes; all were assembled from vacuum interrupter housings. Standard vacuum interrupter materials were used throughout this test series in order to apply product related constraints for the evaluation of feasibility. Vacuum in the  $10^{-5}$  Pa. ( $\sim 10^{-7}$  Torr) range is provided by ion pumps with sorption rough pumping. The cathode consists of various exchangeable vacuum degassed metals. A ring shaped anode surrounds the central cathode coaxially. The anode constitutes a part of the vacuum envelope. The vacuum arc is initiated by a trigger discharge which is established by a voltage surge between an auxiliary trigger electrode and the cathode (See Figure 3). The current is fed coaxially to the test device in order to minimize the magnetic effect of the current return path. The physical set-up is shown in Figure 4.

The vacuum arc discharge, resulting from the trigger spark, burns with about 150V arc voltage until the stored charge is drained from the discharge capacitor bank which serves as a convenient supply of test power. Application of a magnetic field raises the arc voltage substantially. Circuit interruption results if the experimental parameters are chosen properly. Residual voltage remains on the capacitor bank if a circuit interruption is achieved.

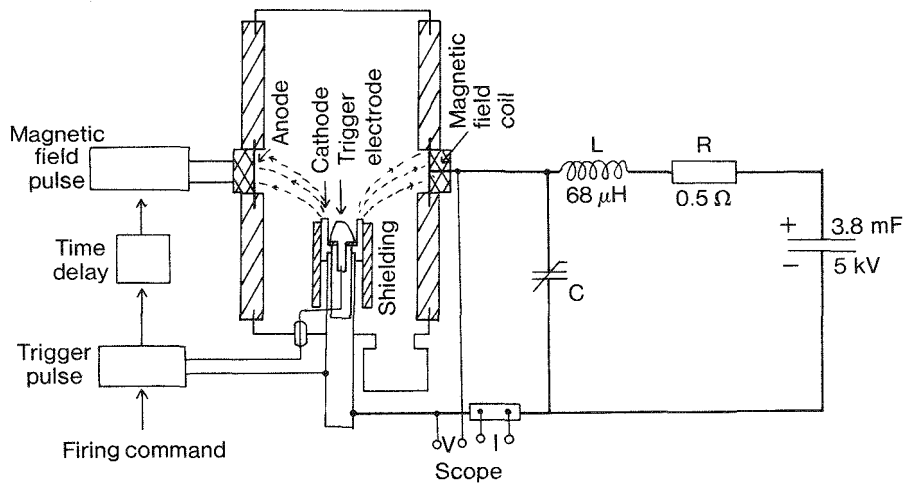


Figure 3. Test Setup for the Magnetically Modulated Vacuum Arc. Power is provided by a Discharge Capacitor Bank.

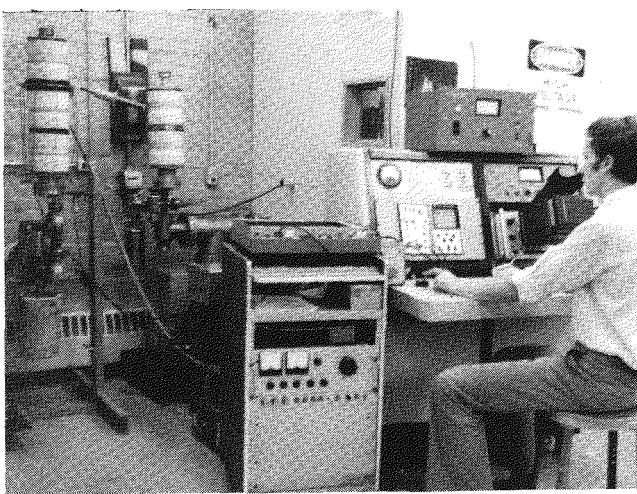


Figure 4. Laboratory Set-Up for Evaluation of Magnetically Modulated Vacuum Arcs. Two Separate Vacuum Systems Allow Fast Change-Over.

### Capacitor Bank Power Supply

The 5 kV, 3.8 mF capacitor bank is housed in the cubicle shown in the right side of Figure 4. This capacitor bank allows convenient, low cost testing in the laboratory. The discharge circuit includes sufficient inductance to simulate conditions for switching on inductive power systems.

The magnitude and shape of the discharge current and the transient circuit recovery voltage following an interruption are controlled by air core inductor L and resistor R. Further capacitance C is placed in parallel to the discharge device as an experimental variable. The pulse shape of the test current is determined by the total circuit inductance, resistance and the 3.8 mF capacitance of the capacitor bank. The frequency of the recovery voltage oscillations is determined by the parallel capacitance C and the circuit inductance L. Capacitance C is charged in parallel with the capacitor bank. Upon triggering of the vacuum device, an oscillatory inrush current is created which is determined by capacitor C and the distributed inductance between C and the vacuum device. (About 2.0  $\mu$ H). The inrush current often crosses the zero line which can lead to premature recovery of the vacuum gap. In this case only a short pulse of current is conducted. This problem is overcome by extending the length of the trigger pulse.

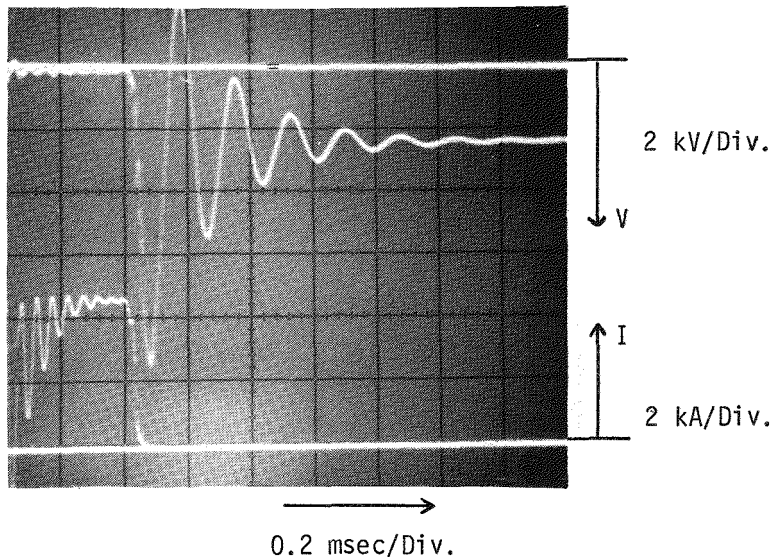


Figure 5. 4.5 kV Vacuum Arc switched off by the application of a 59 mT magnetic field pulse. Copper Cathode. 11.4  $\mu$ F of capacitance parallel to the vacuum device.

Magnetic switching is initiated after the oscillatory inrush current has been damped out. A typical switching operation is shown in Figure 5. 0.4 msec after initiation of the 4.5 kA vacuum arc, a magnetic field is applied which drives the arc current toward zero. The peak transient recovery voltage is 9.5 kV.

#### Magnetic Control Field

The magnetic control field is generated by discharging a capacitor into a winding of about 10 turns of well insulated wire which surrounds the anode.

The anode acts as a short-circuited winding to the pulsed magnetic field coil. The magnetic field pulse diffuses through the anode as described in the following partial differential equation.

$$\nabla^2 \vec{B} = \mu \sigma \frac{\partial \vec{B}}{\partial t}$$

With  $\vec{B}$  = magnetic field strength.

$\mu$  = magnetic permeability.

$\sigma$  = electrical conductivity.

$t$  = time.

The associated time delay  $\tau$  can be estimated by inserting characteristic variables.

$$\tau = \mu \sigma d^2$$

With  $d$  = anode wall thickness.

$\tau$  = typical time delay of the magnetic pulse diffusing through the anode metal, flat plate approximation.

An example of a magnetic field calibration is shown in Figure 6. The lower trace is obtained from a calibrated search coil placed inside the anode. The upper trace shows the exciting current flowing through the winding on the outside of the anode. Diffusion delays the peak of the magnetic field by 51  $\mu$ sec beyond the peak of the current.

The time delay can be varied over a wide range by properly choosing the anode wall thickness, conductivity and permeability of the material.

The magnetic field can either be excited from a separate power supply with electronic control for timing or from the anode current through a series connected winding. In the latter case, the diffusion time delay can replace the electronic timing control. Anode geometry and material can be designed for a time delay up to a millisecond. The series connected winding simplifies the system considerably.

The stated magnetic field strength applies to the inside of the ring-shaped anode. The value on the axis is lower.

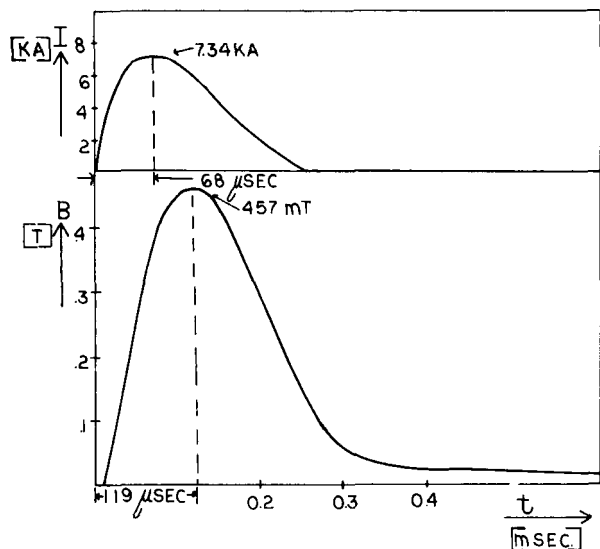


Figure 6. Magnetic Field Pulse inside the Ring Anode and Excitation Current in 8 Turn Coil surrounding the Anode.

### Triggering

Reliable triggering is essential to the feasibility of the vacuum arc commutator. The basic trigger options are reviewed in Appendix B. A surface discharge across an insulating surface was chosen for triggering the vacuum arc. This represents a hybrid between a field emission and an exploding metal film trigger. In an early phase of the project this scheme was optimized for the given application.

The original trigger electrode surrounded the cathode, held in place by a ceramic sleeve. It was difficult to prevent attachment of the main discharge to the trigger lead wire. (See Figure 7). Various methods of shielding the trigger lead proved unsatisfactory.

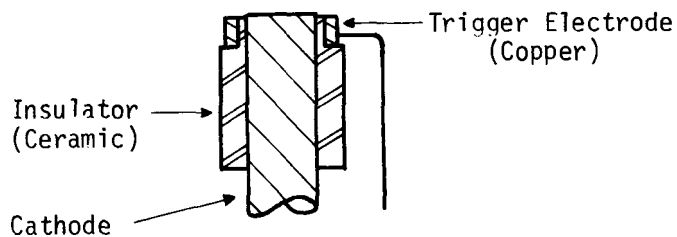


Figure 7. Trigger Arrangement used in early phase of the work.

Perfect shielding of the trigger lead wire can be provided if mounted on the axis of a cylindrical cathode. This arrangement proved to be most successful. (See Figure 8). Further it was found that a graphite trigger electrode provided longer life than a metallic one.

Trigger energy was derived from a charged capacitor switched with a triggered spark gap. (See Figure 9).

About 3 kV charging voltage on the 15  $\mu$ F trigger capacitor was needed to attain reliable firing for anode-cathode voltages near 100V. The observed time delay between trigger discharge and start of the vacuum arc was under 10  $\mu$ sec. typically at 5  $\mu$ sec. For reasons not connected with the vacuum device, most testing was conducted with 6 to 8 kV on the trigger capacitor, leading to a critically damped trigger current of about 2 kA. Conducting layers on the insulator surface between trigger electrode and the cathode are needed for successful firing. Metal vapor deposited from the vacuum arc generates the conducting layers. On a virgin surface the conducting layer was provided by pencil marks, applied before assembly. Erosion on insulator and copper-trigger

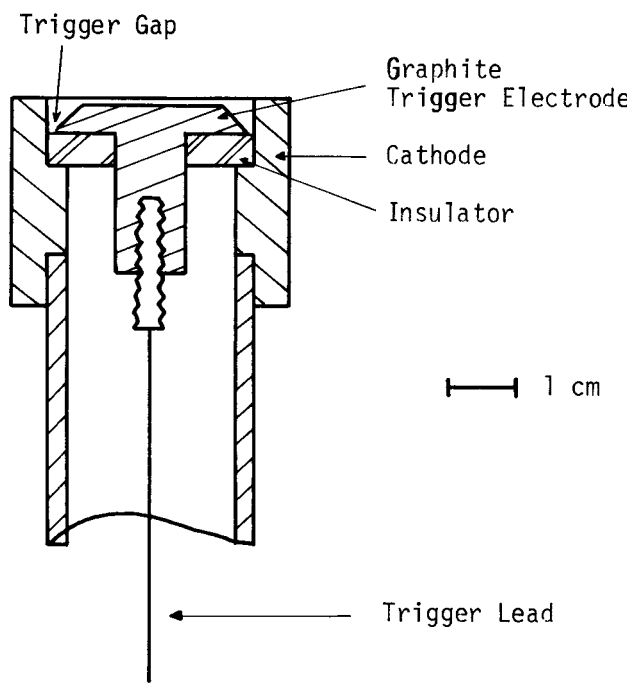


Figure 8. Graphite Trigger Electrode Mounted Internally of Tubular Cathode.

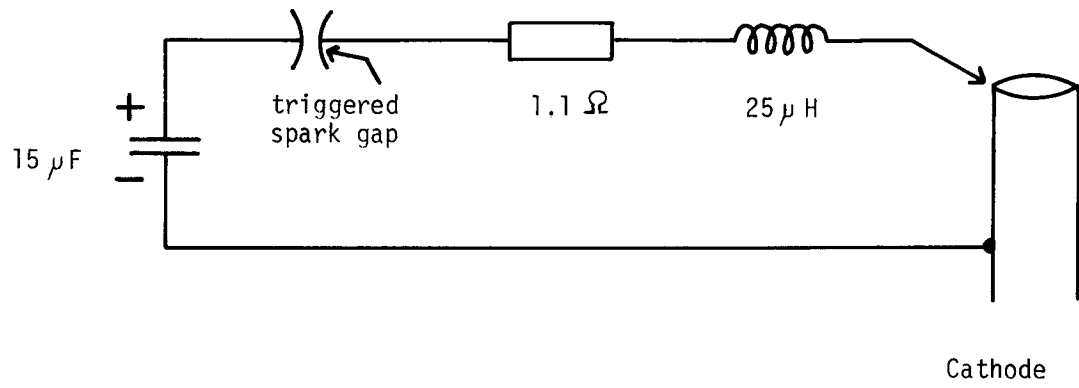


Figure 9. Diagram of Trigger Circuit.

electrode is particularly heavy for a main cathode made from refractory metals, such as tungsten, molybdenum or tantalum. This leads to a need for increased trigger voltage after about 50 discharges. A trigger electrode made from graphite showed much less erosion. Various test sequences up to about 300 discharges were completed without trigger failure. Either boron nitride, or Corning machineable glass-ceramic were found to be suitable materials for the insulator between the trigger electrode and the cathode.

#### Measurements

The vacuum pressure level was determined either from an ionization gauge or from the current reading of the calibrated ion pump.

Current was measured with a coaxial shunt of 1.0 mΩ resistance and an inherent rise time of 180 nanosec. Voltages were measured through a Tektronix 1000X voltage divider with a rise time of 7 nanosec. Two oscilloscopes with flat frequency response up to 500 KHz were used for data acquisition. (Hewlet-Packard 132 A Dual Beam and Nicolet Digital, Explorer II).

## PARAMETRIC STUDIES

From prior work it was known that the vacuum arc discharge can be switched off by the application of a transverse magnetic field. (1). The objective of the described project is to improve the understanding of the physics involved and to optimize the switching performance for a given application. Experiments were conducted in order to answer the following questions:

- What mechanism creates high vacuum arc voltages when the transverse magnetic field is applied?
- Find an optimum geometry, trigger-arrangement, and cathode material.
- Determine the effect of residual pressure level, anode area and parallel capacitance.

### Discharge Geometry

Gilmour (1). showed that the transverse magnetic field could be applied most effectively to a geometry where the anode coaxially surrounds the cathode. This was corroborated by testing a geometry with plane parallel electrode surfaces. This did show a reduced switching performance. Gilmour arranged the magnetic field coil inside the vacuum vessel, requiring current feed throughs. This arrangement was complex in construction, and it was very difficult to shield the current feed throughs from spurious current attachment from the arc plasma. Consequently, we made a metallic section of the vacuum envelope to act as the anode. The magnetic field coil is wound onto the outside of the anode. This eliminates the need for current feed throughs to the anode or magnetic field coil. The basic arrangement is shown in Figure 3. The ability to generate high arc voltages when the magnetic field is applied is a measure of switching performance. An axial offset of 2 to 5 cm between anode and cathode was found to be an optimum range. A test series with cathodes of extended length showed a reduced switching performance. The cathode end surface should not protrude more than a few mm beyond the surrounding insulating surfaces. From the point of device life and freedom of design it is desirable to use extended cathodes. But the tests showed that the switching performance suffers if cathode areas are directly opposite from anode areas, so that cathode vapor jets can blast directly at the anode. High arc voltage is related to low plasma density in front of the anode. This can best be attained if the cathode vapor jets do not point at the anode. Further, it is observed that high arc voltage is accompanied by a large amplitude of high frequency oscillations on the arc voltage.

Further it was found that the cathode spot velocity was under 100 m/sec, which limited most of the cathode attachment to the vicinity of the trigger spark. Also this fact limits the useful extension of the cathode to a few cm beyond the trigger area.

All further testing was performed with cathodes protruding no more than 2 mm beyond the surrounding insulator surface.

The anode consisted of essentially straight stainless steel cylinders, welded between the metal inserts of the glass ceramic housing. One deviation from the straight anode geometry was tested which was stimulated by a similar geometry described as most successful in Gilmour's earlier publication (1). See Figure 10. The switching ability of the indented anode turned out to be less than for the basically straight cylindrical design.

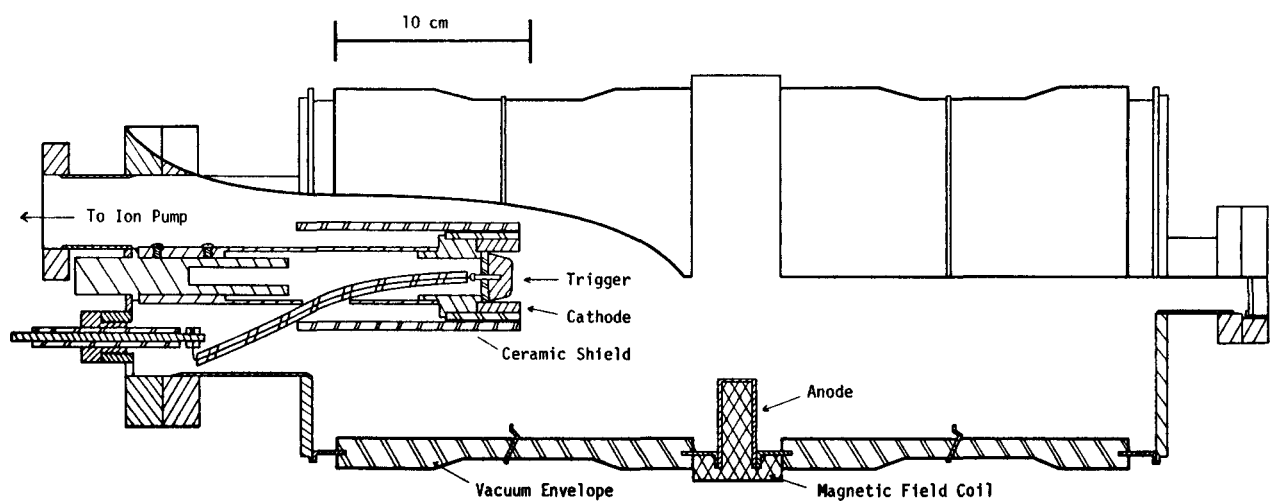


Figure 10. Anode Geometry with Indented Stainless Steel Surface.

### Residual Vacuum Pressure

Following exposure to the atmosphere the demountable test chambers are baked to 200°C under vacuum in order to remove a large fraction of the surface gases.

Further removal of surface gases is brought about through repeated arcing.

Figure 11 shows the peak pressure reached during each arc discharge.

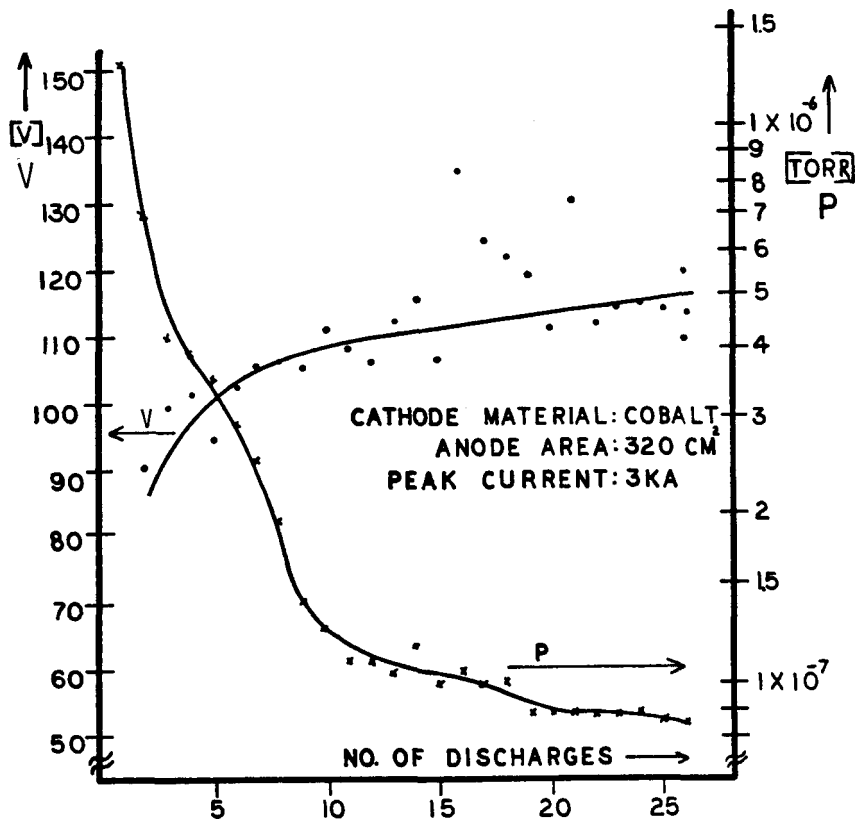


Figure 11. Arc Voltage (at 3 kA) and Pressure Rise During Clean-Up Discharges in the Demountable Test Chamber.

The pressure is measured within the ion pump. The actual pressure in the discharge chamber will be higher. Figure 11 shows the removal of surface gases as indicated by a falling pressure with successive vacuum arcs. The arc voltage rises correspondingly. Further it is observed that the switching ability increases after a number of clean-up discharges have been fired. These observations are in

agreement with theories described in the literature which predict that the plasma sheath near the anode depends on the local gas density. The steady pressure before discharging is in the  $10^{-7}$  Torr range.

One test device, constructed with all metal seals, was baked to  $450^{\circ}\text{C}$  for 8-hrs. in order to determine whether the gas loading is a performance limiting factor. This device incorporated beryllium electrodes. (See Figure 12)

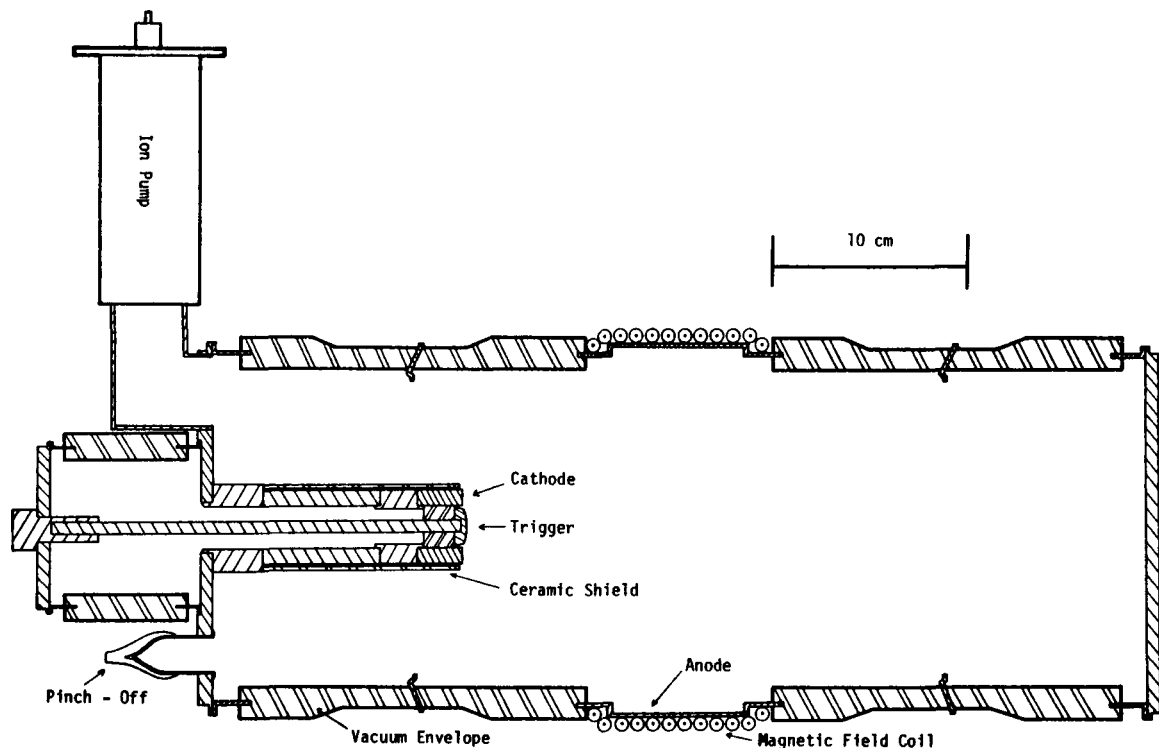


Figure 12. Test Device with all welded and brazed Joints.  
Baked at  $450^{\circ}\text{C}$  for 8-hrs. before pinch-off.

The switching ability was equivalent to its demountable counterpart with a Viton seal. It appears that a number of conditioning discharges in a demountable ion-pumped device are just as effective in removing surface gases as a hard bake of the device.

### Cathode Materials

The selection of cathode materials was guided by the following parameters:

- Availability and price
- Low Vapor Pressure
- Machineability
- Ability to be joined to copper
- Triggerability
- Low Arc Voltage without magnetic field
- High Arc Voltage with magnetic field applied
- Rapid dielectric recovery following current switch-off (switching ability)

An early phase of the project evaluated various vacuum cast cathode materials in the form of 1 cm diameter cylinders. These were mounted in a holder and surrounded by a concentric trigger electrode. Ceramic shielding was applied to the holder and the trigger leads in order to restrict arc attachment to the cathode material. (See Figure 13)

The test chamber is assembled from three standard vacuum interrupter housings which are welded together end-on. The anode consists of stainless steel with a total surface area of  $320 \text{ cm}^2$ . The anode is surrounded by an eight turn coil for generating the magnetic control field. A pump-out port connects the test chamber to a 500  $\text{l/sec}$  ion pump which maintains the pressure in the  $10^{-7}$  Torr region. The parallel capacitance was  $0.04 \mu\text{F}$ .

Measured values of arc voltage as a function of current and magnetic field strength are summarized in Table I. High frequency noise of about 100 to 200V amplitude was found to be superimposed on the voltage traces. High arc voltage is associated with high noise amplitude.

Beryllium and cobalt became available only in a later phase of the project.

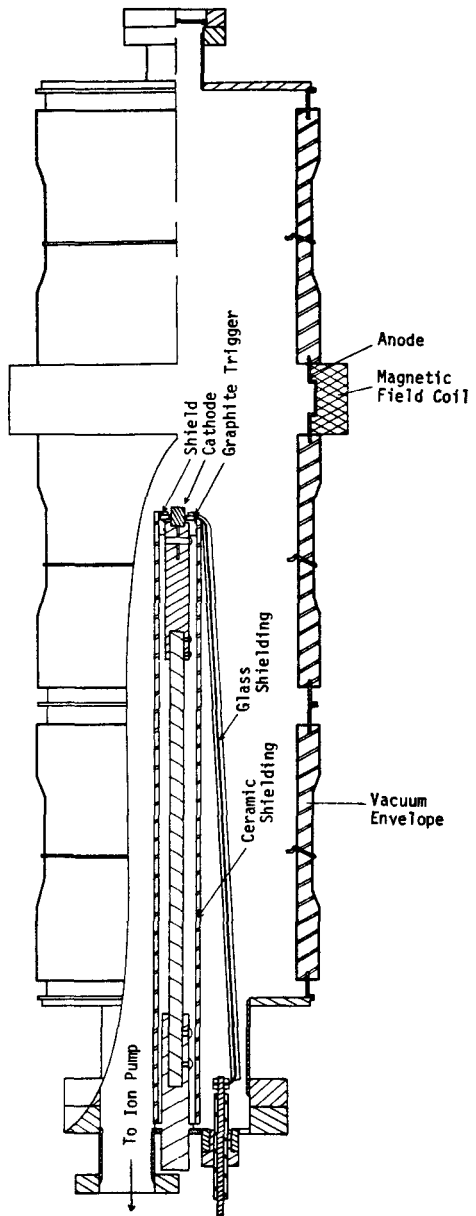


Figure 13. Test Device for Evaluation of Cathode Materials.

These materials were tested in the form of a 3.8 cm outer diameter cylinder with internal trigger electrode. (See Figure 14)

Table I  
AVERAGE ARC VOLTAGE FOR VARIOUS CATHODE MATERIALS

<u>Cathode Material</u>	<u>B=0 2 kA (Volt)</u>	<u>B=0 3 kA (Volt)</u>	<u>B=0 4 kA (Volt)</u>	<u>B=0 5 kA (Volt)</u>	<u>B=134mT 3 kA (Volt)</u>	<u>Amplification Factor</u>
Aluminum	300	200	200	250	800	4.0
Silver		150	170	150	520	3.5
Chrome		200		180	680	3.4
Titanium		200	180	220	900	4.5
Iron		200	200	180	500	2.5
Nickel	250	200	240	200	820	4.1
Copper	200	250	280	290	760	3.0
Molybdenum	190	180		220	800	5.0
Graphite	150	200		200	550	2.8
2% Thoriated Tungsten	170	170		180	580	3.4
Tungsten	170	200		220	700	3.5
Vanadium	130	140		200	680	4.8
Tantalum	150	170	200	200	600	3.5
Niobium	180	200		230	760	3.7

The arc voltages without applied magnetic field are substantially higher than for electrodes with opposing surfaces. Smaller anode area leads to higher values. Anode voltages up to several kV have been observed for an anode area of  $230 \text{ cm}^2$  and below. This tendency is particularly pronounced for metals with a low atomic weight and a high melting point, such as beryllium, chromium, vanadium, titanium and aluminum. This so-called self-limited mode of the vacuum arc is of no particular interest to the objective of this project. But it is important for understanding the mode of operation.

The amplification factor in Table I is defined as the ratio of arc voltage with and without applied magnetic field of 134 milli Tesla. The most effective arc voltage amplification was obtained for molybdenum, vanadium, titanium and nickel. Also, cobalt was later shown to have a high value.

During the cathode material study the following materials displayed an interruption ability of 3 kA with 134 milli Tesla applied: aluminum, titanium, nickel, copper and tungsten. The lowest switching ability was shown by silver (2.4 kA), thoriated tungsten (2 kA) and graphite (below 2 kA).

In conclusion, a wide choice of cathode materials is available. Further studies were conducted with aluminum, copper, tungsten, molybdenum, cobalt, beryllium, vanadium, niobium, and titanium. Considering the availability in vacuum degassed quality the following materials appear as a practical choice: copper, aluminum, cobalt, titanium, nickel and the refractory metals.

#### Potential Distribution

Floating potential measurements were taken on all available metallic inserts which are in contact with the plasma. Locating the potential distribution in the plasma is important for understanding the operation of the device. The left side of Figure 14 lists the measured floating probe potentials without applied magnetic field. The right side lists the values with 0.26 Tesla of magnetic field applied to the anode. The arc current is 3 kA.

The measured values show that the potential drop is concentrated in the area of the anode where magnetic field lines and the flow of current cross each other at right angles. Application of the magnetic field strongly raises the anode potential. The end plate is close to the cathode potential. These observations agree with those made by Knauer on the Penning discharge (2). (3). Applying the magnetic field raises the arc voltage and also introduces high frequency components. The floating potential at positions remote from the anode can even be reduced by the applied magnetic field.

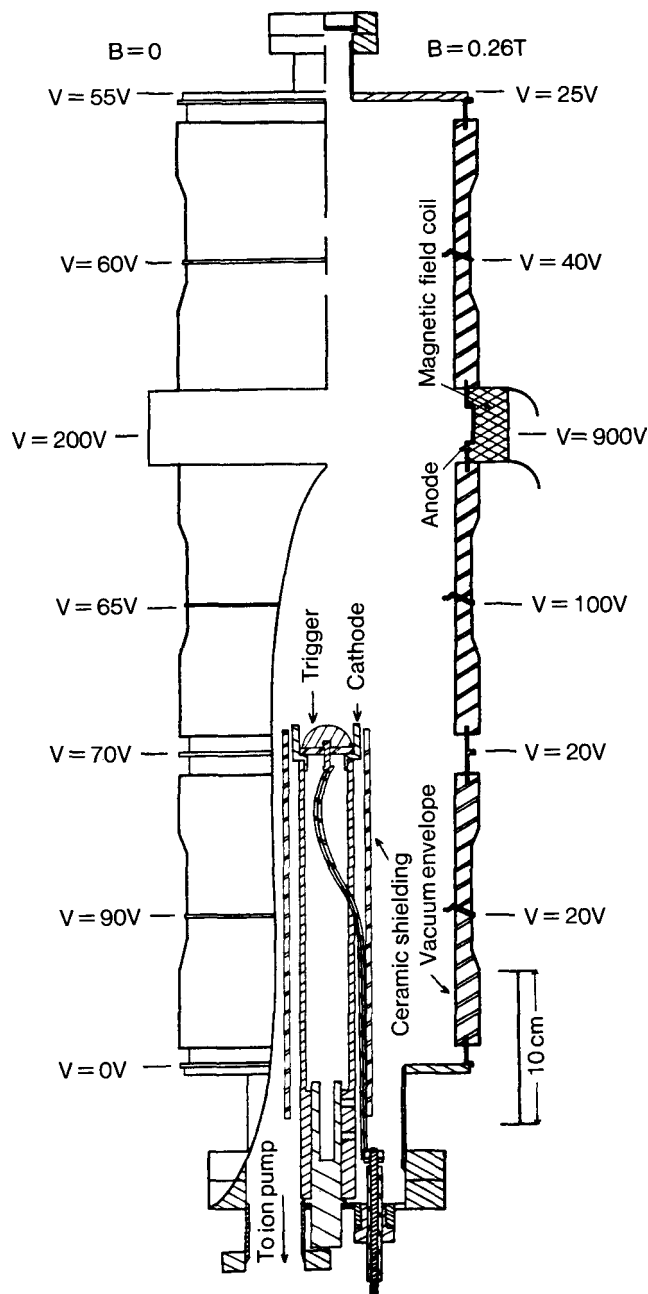


Figure 14. Coaxial Discharge Geometry with Axially Offset Cathode. Values of Floating Plasma Potential are shown for 3 kA of Arc Current. Left side for Vacuum Arc without Magnetic Field. Right side for 0.26 Tesla of Magnetic Field applied.

The following two oscilloscopes illustrate the described facts.

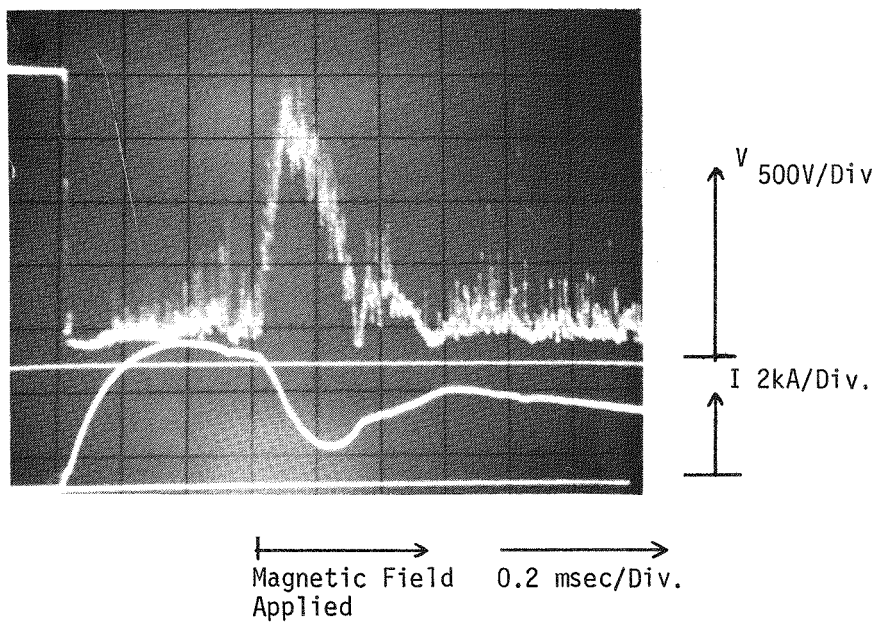


Figure 15. Application of 0.58 Tesla Magnetic Field Increases Anode Voltage to about 2.2 kV above Cathode Potential.

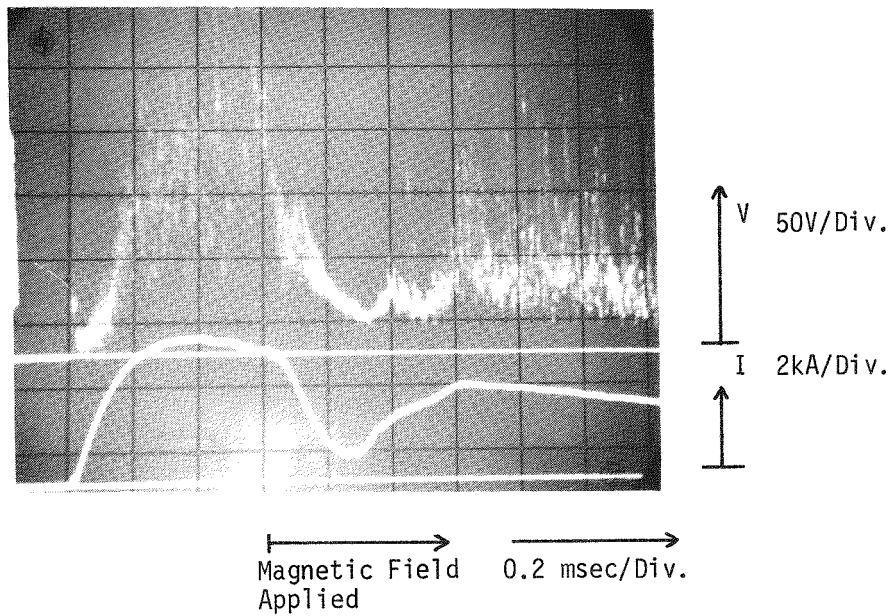


Figure 16. Application of 0.58 Tesla Magnetic Field reduces Potential at Top Plate of Vacuum Envelope (See Figure 14) to only 25 volt above Cathode Potential.

Further it was attempted to use the metal inserts as Langmuir Probes. Langmuir Probes are metal probes in contact with the plasma, which can collect ions with a negative bias voltage applied and electrons with a positive bias applied. In principle these measurements are useful because plasma densities and electron temperature can be derived from such measurements.

We found that the metal insert probes were drawing hundreds and thousands of amperes of current due to their large area. These currents perturbed the plasma to be measured. The ion saturation current could not be distinguished from the establishment of cathode spots on the probes. Smaller probes could have been inserted if the test envelopes were suitably rebuilt. This topic was not pursued further because it is not in the main line of establishing feasibility for practical devices.

#### Microwave Measurements

In cooperation with R. Dollinger of SUNY X-band microwaves were used for determining the density of the electrons within the magnetically modulated vacuum arc. The electron density, averaged over the diameter, is about  $10^{12} \text{ cm}^{-3}$  at 6 kA of current. The electron density varies with the arc current. The average electron density is not affected by the magnetic field. One can assume that the magnetic field focuses the cathode plasma stream, so that the average density stays constant while the electron density near the anode is reduced.

### Effect of the Magnetic Field

Magnetic modulation of vacuum arcs requires the application of a magnetic field perpendicular to the flow of arc current. Most effective is an axi-symmetric electrode arrangement where a closed-ring Hall-current can be established in the plasma.

The magnetic field is generated by a current carrying coil wound directly onto the outside of the anode. Magnetic field windings, wound onto the vacuum envelope axially offset from the anode, were found to be less effective.

The applied magnetic field raises the arc voltage and simultaneously excites high frequency oscillations. See Figure 17.

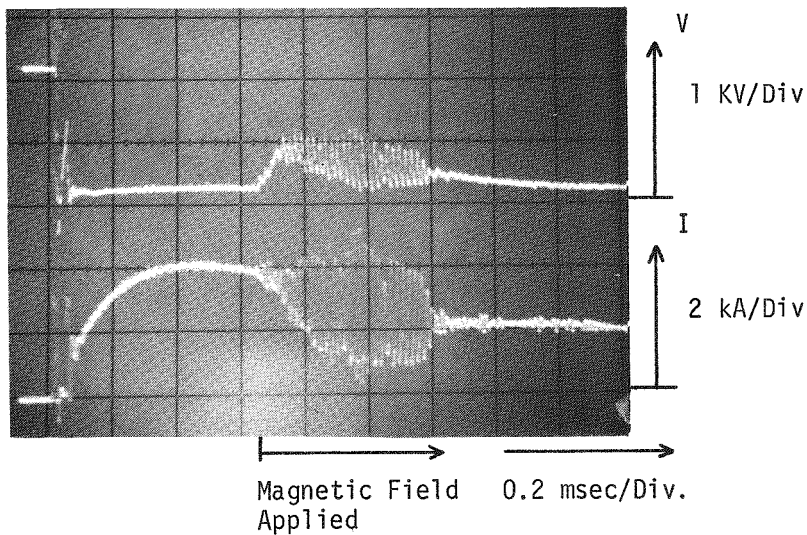


Figure 17. Magnetic Field Pulse raises the Vacuum Arc Voltage and excites High Frequency Oscillations. Peak Magnetic Field Strength 27 milli Tesla. Copper Cathode. Parallel Capacitance 7.64  $\mu$ F.

The magnetic field strength determines the magnitude, but not the frequency of the oscillations during the magnetic modulation.

This observation rules out a rotating current spoke as the source of oscillations. The frequency of a rotating instability would grow with the magnetic field strength.

Further, it is observed that the frequency of the oscillations scales with the  $-1/2$  power of the shunt capacitance applied to the vacuum device. This shunt capacitance  $C$  is charged together with the capacitor bank. Upon triggering of the vacuum arc, the shunt capacitor will discharge through the vacuum arc. The inductance of the shunt capacitor - vacuum device circuit is about  $2 \mu\text{H}$ . The vacuum arc starts with a damped oscillation which is controlled by the value of shunt capacitance and circuit inductance and resistance. The oscillations, excited by the magnetic field, are identical in frequency with the current inrush oscillations. These oscillations exchange energy between the vacuum device and the shunt capacitor. It is suggested that this is related to an oscillating electron space charge sheath in front of the anode.

Oscillating arc discharges have already been used in the pioneering days of radio transmission. It is a new observation that magnetic modulation of vacuum arcs allows a convenient control of oscillations.

A later section analyzes the criterion for the existence of oscillations. DC circuit switching can be obtained when the magnetically induced oscillations bring the arc current toward zero. For a clean vacuum system, dielectric recovery will follow with a high  $dv/dt$  capability.

Magnetic modulation of the vacuum arc impedance is demonstrated in Figure 18. 0.5 msec after start of the discharge, a magnetic field pulse of 0.62 Tesla peak magnitude is applied to a 4.5 kA vacuum arc. For the duration of the magnetic field pulse, the arc voltage is raised from 300V to a peak of 1,800 V. Shut-off does not occur with this particular test shot because the current is not reduced sufficiently.

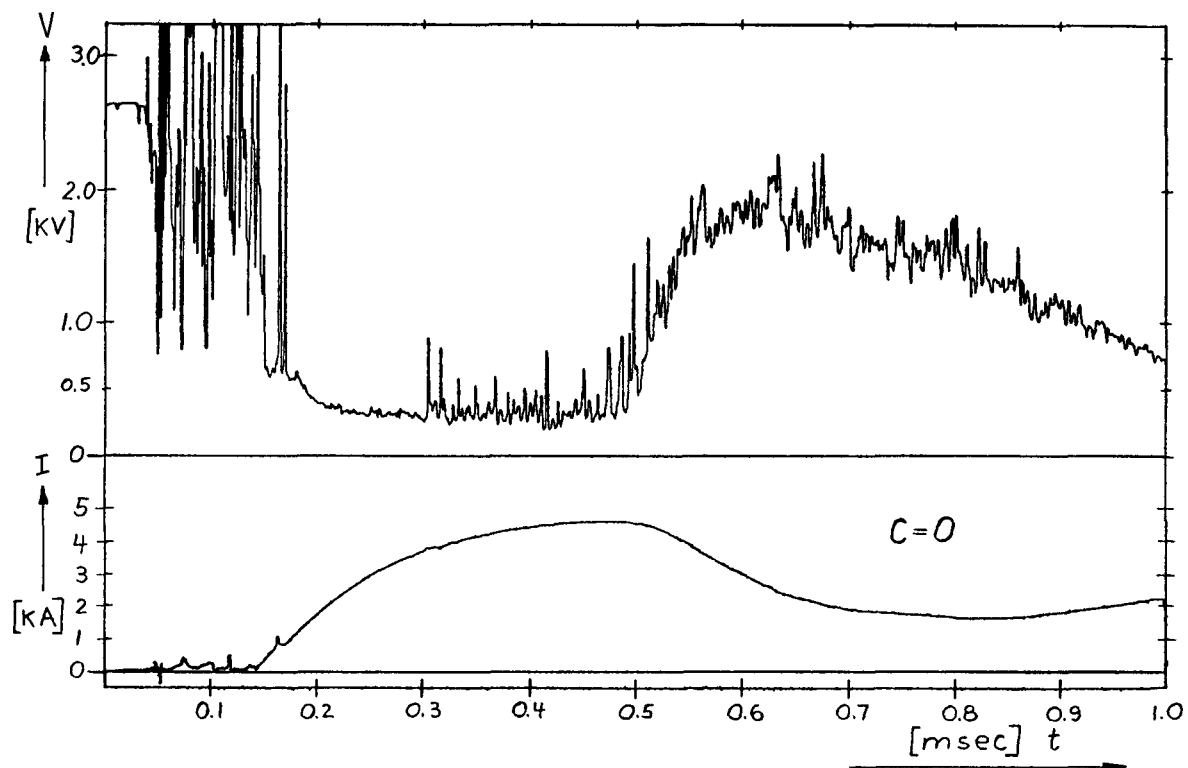


Figure 18. Elevation of Arc Voltage due to an applied Magnetic Field of 0.62 T Peak Magnitude with Aluminum Cathode. Anode area  $320 \text{ cm}^2$ .

A summary of magnetic modulation data is shown in Figures 19 and 20. The vacuum arc impedance as derived from noise averaged values of arc voltage and arc current is shown as a function of the instantaneous magnetic field strength. The data are derived from oscillograms similar to Figure 18. The parameter is the arc current.

The stated magnetic field strength applies to the inside of the ring-shaped anode. The value on the axis is about 37% lower.

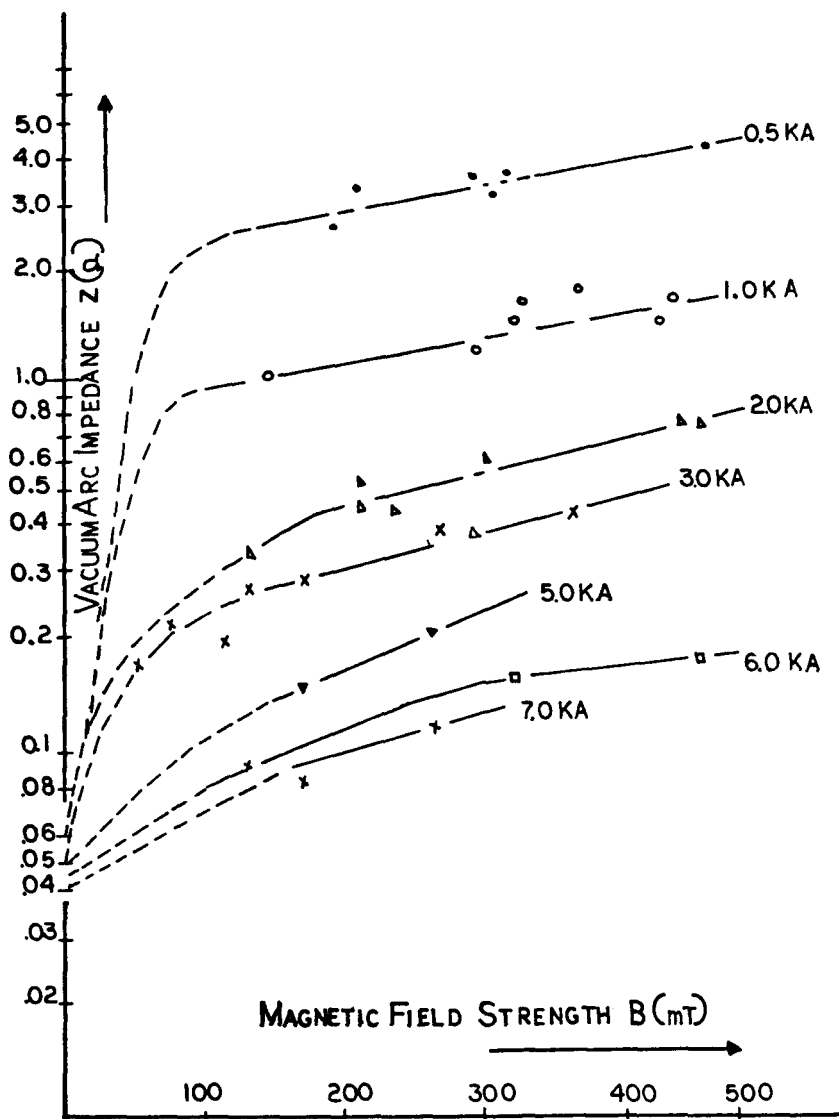


Figure 19. Vacuum Arc Impedance as Function of Magnetic Field Strength. Parameter is the Arc Current. Molybdenum Cathode with Ring Anode of  $320 \text{ cm}^2$  Area. Pressure  $10^{-7}$  Torr Range.

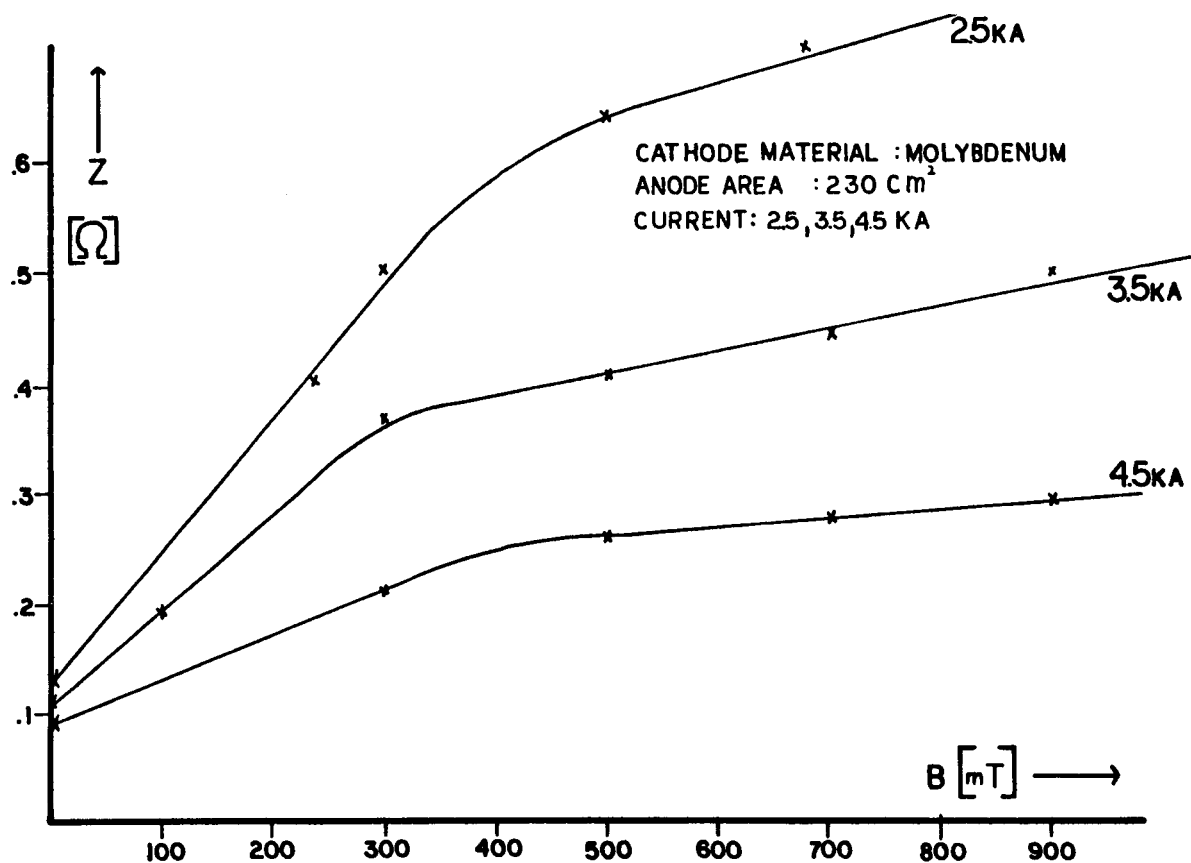


Figure 20. Vacuum Arc Impedance as Function of Magnetic Field Strength.

#### Vacuum Arc Impedance

The vacuum arc voltage without applied magnetic field is typically between 150 and 300 volts for the coaxial geometry where the cathode vapor jets do not impact on the anode. Higher arc voltages up to several kV have been observed for metals like beryllium, aluminum, titanium and cobalt. This so-called self-limited mode of the vacuum arc has been investigated in greater detail by Dollinger and Gilmour under Contract RP-476-1. The self-limited mode is associated with strong high frequency noise on the arc voltage. This mode only occurred for small anode areas of  $230 \text{ cm}^2$  and below. This phenomenon was not investigated further because it is not of interest to the application at hand, the commutating switch.

The arc impedance as a function of current for various cathode materials is shown in Figure 21. The vacuum arc impedance without applied magnetic field is only weakly dependent on current. The corresponding voltage - current characteristic is either flat or positive.

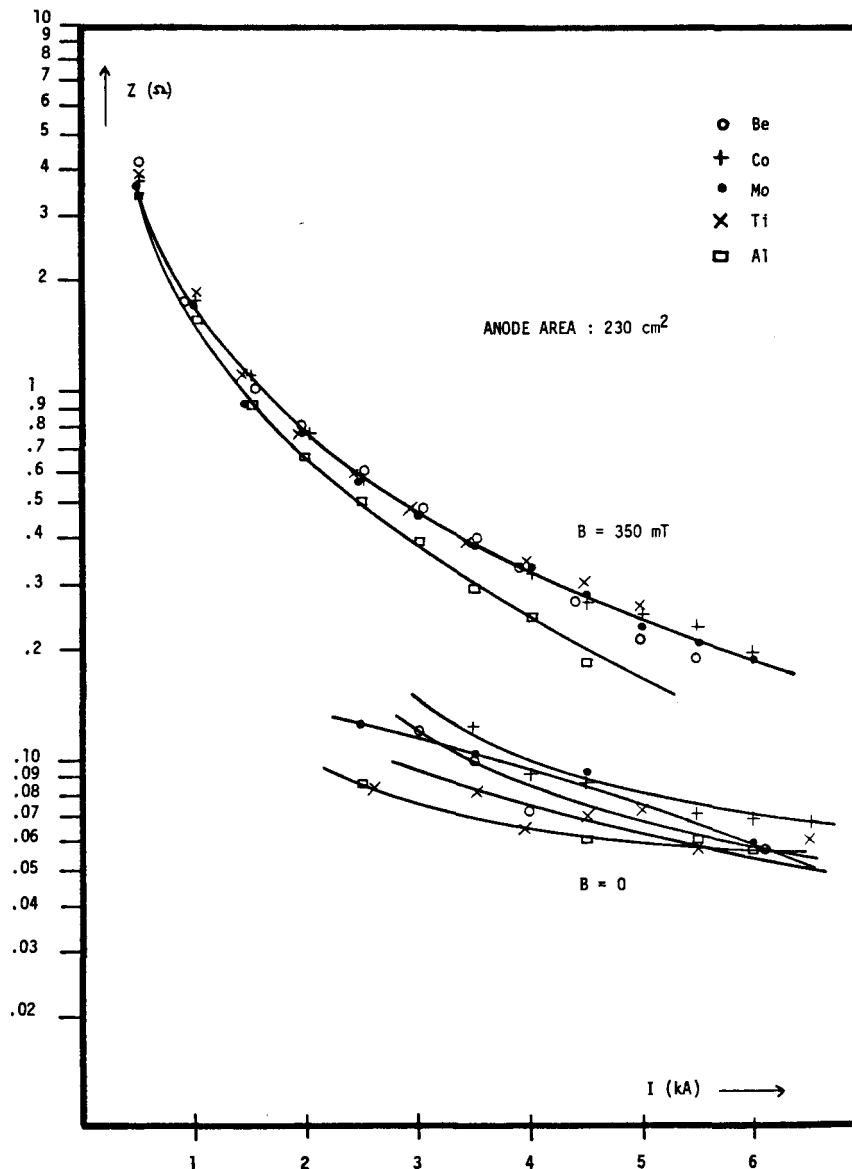


Figure 21. Arc Impedance as Function of Current for Various Cathode Materials With and Without Applied Magnetic Field.

The vacuum arc impedance falls off rapidly with increasing current when the magnetic field is applied. The corresponding voltage-current characteristic is negative. In other words, applying the magnetic field transforms the vacuum arc into the region of negative voltage - current characteristics. This fact will be used later in the evaluation of switching theory.

Similar curves with varied magnetic field strength are shown in Figure 22. A saturation effect is apparent where increases in magnetic field strength lead to a diminishing increase in vacuum arc impedance. Progressively larger magnetic fields are required to achieve magnetic modulation at higher arc currents. Lower values of vacuum arc impedance are observed for anodes with larger surface area. This observation points toward the anode current density as a critical parameter.

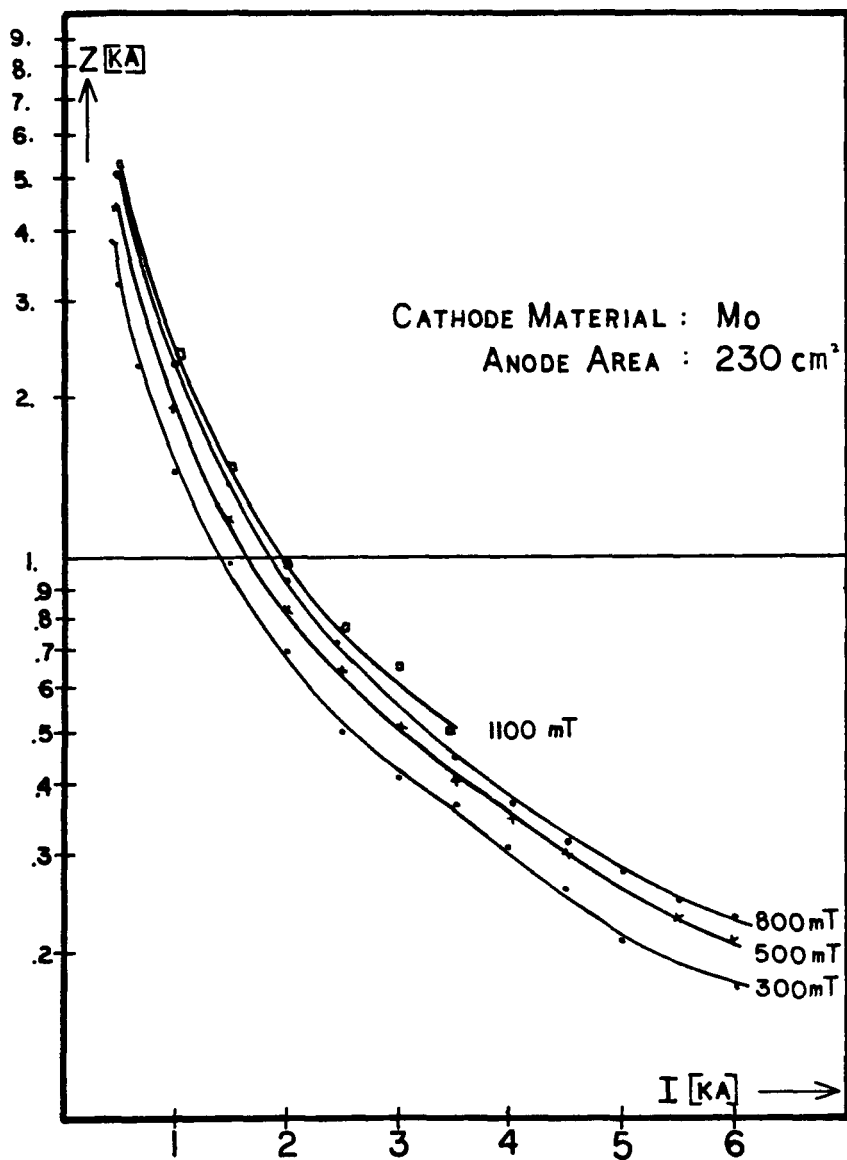


Figure 22. Arc Impedance as Function of Current for Different Magnetic Field Strength.

### Circuit Interruption Tests

DC switching can be obtained due to the increased arc impedance and due to the induced oscillations which bring the arc current toward zero. For a clean vacuum system, dielectric recovery will follow with a high dv/dt capability. Adding parallel shunt capacitance to the vacuum device increases the switching ability. See Figure 23.

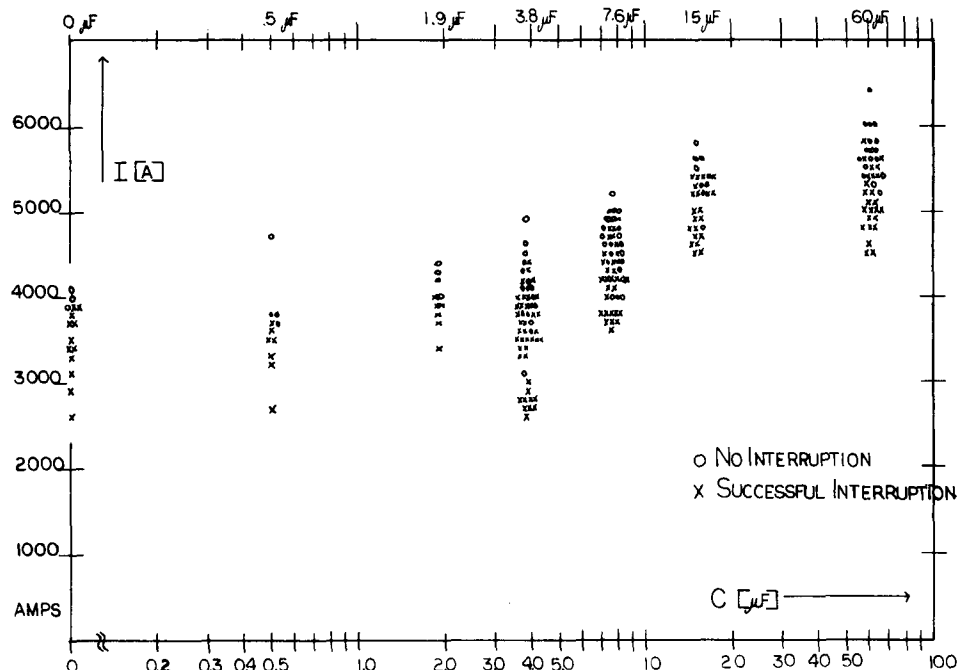


Figure 23. Interruption Ability of the Magnetically Modulated Vacuum Arc as a Function of the Parallel Capacitance with Molybdenum Cathode and Anode Area of  $690 \text{ cm}^2$ . Peak Magnitude of Applied Magnetic Field 0.37 Tesla.

60  $\mu$ F of capacitance placed parallel to the vacuum device increases the switching ability by a factor of about 2. Applied parallel capacitance changes the mode of switching from a slow ramp-down of the current to a fast oscillatory decrease.

The highest switch-off ability so far attained was 9 kA with a peak recovery voltage of 6 kV. The parallel capacitance was 157  $\mu$ F with a magnetic field strength of 97 mT applied, using a molybdenum cathode. The 9 kA current value represents a limit that we were not able to exceed with the given geometry. The voltage of 6 kV was the limit of the power supply. Voltage recovery to substantially higher values is possible, as shown in later 60 Hz Power Lab Tests.

The switching behavior with and without parallel capacitance is illustrated in Figures 24 and 25. The vacuum discharge geometry of Figure 14 was employed for this test series.

Figure 24 shows switch-off without applied capacitance. The cathode consists of vacuum degassed aluminum which tends to go spontaneously into the high impedance mode without applied magnetic field. This is evidenced by short voltage spikes and corresponding current reductions before the magnetic field is applied at the 0.5 msec time mark. The current decreases linearly and reaches zero at about the time when the magnetic field reaches its peak of 0.62 Tesla. The shape of the arc voltage can be explained considering the given decrease of current and the test circuit constants.

Switching under similar conditions, with 15  $\mu$ F of parallel capacitance applied, is illustrated in Figure 25. The parallel capacitance leads to an inrush current oscillation, which is damped out at the 0.2 msec time mark. The magnetic field is applied at the 0.5 msec time mark, leading to rapid switch off for the current. Oscillations are already present before the magnetic field is applied. This is not typical. In most cases the oscillations start when the magnetic field is applied, leading to switch-off when the current attempts to cross the zero line. The recovery voltage oscillates if parallel capacitance is applied.

Figure 26 demonstrates the increasing interruption ability with increasing magnetic field strength. The tests are performed without parallel capacitance. The available source voltage is limited to 5 kV, corresponding to the maximum voltage charge on the capacitor bank used as power source. The series inductance in the test circuit is 68  $\mu$ H.

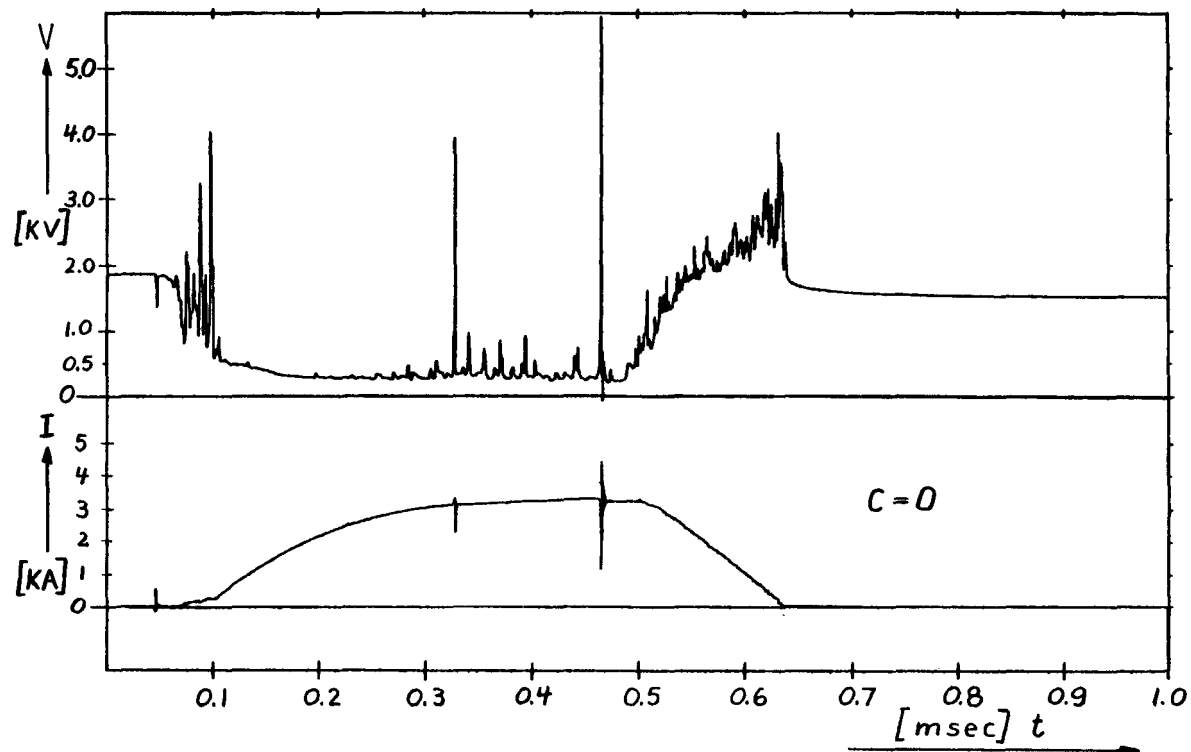


Figure 24. Vacuum Arc switched off by Magnetic Field of 0.62 Tesla  
 Peak Magnitude. Aluminum Cathode with Anode Area of  $320 \text{ cm}^2$ . No  
 Parallel Capacitance applied. Current decreases steadily toward zero.

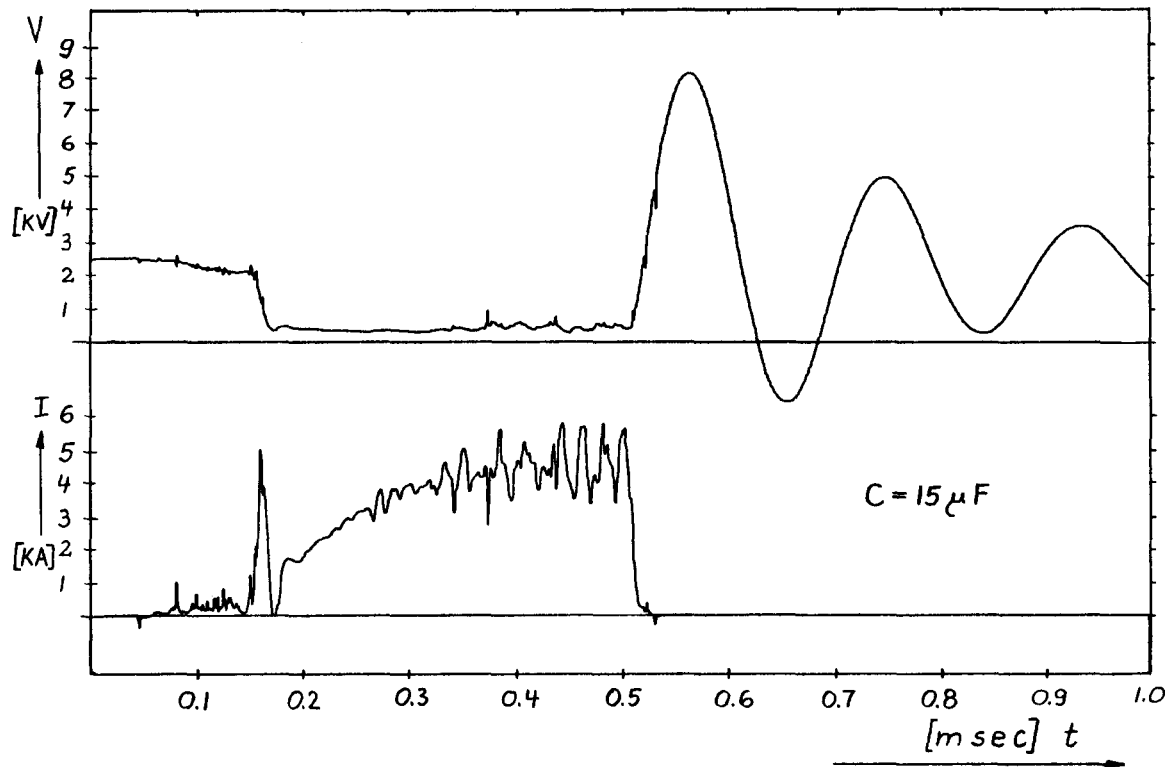


Figure 25. Vacuum Arc switched off by Magnetic Field of 0.62 Tesla Peak Magnitude. Aluminum Cathode with Anode Area of  $320 \text{ cm}^2$ . Parallel Capacitance of  $15 \mu \text{F}$  applied. Current decreases abruptly to zero.

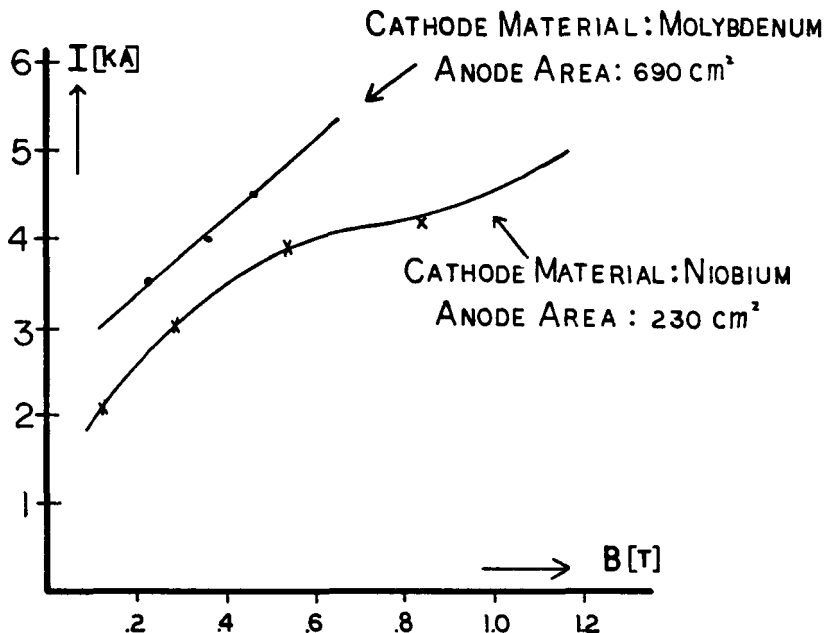


Figure 26. Interruption Ability as Function of Magnetic Field Strength Without Parallel Capacitor.

Increased anode area leads to increased interruption ability. Test data obtained with 15  $\mu$ F of parallel capacitance are shown in Figure 27. The anode area was changed by varying the length of 7.5" diameter cylindrical anodes. Larger anode area corresponds to lower magnetic field strength since the same power supply was used to generate the magnetic field.

Increasing the anode area by increasing the diameter should be more effective than changing the length because increased diameter leads to reduced plasma density in front of the anode. We know that a smaller anode diameter leads to reduced interruption ability. Anodes with a diameter above 7.5" were not tested due to rescheduling of this project.

A wide choice of cathode materials is available. The interruption ability of nine metals is listed in Table II. The variation within this group is about 20%. Cobalt and beryllium show the highest interruption ability. Also

copper which is readily available in degassed form has comparable performance.

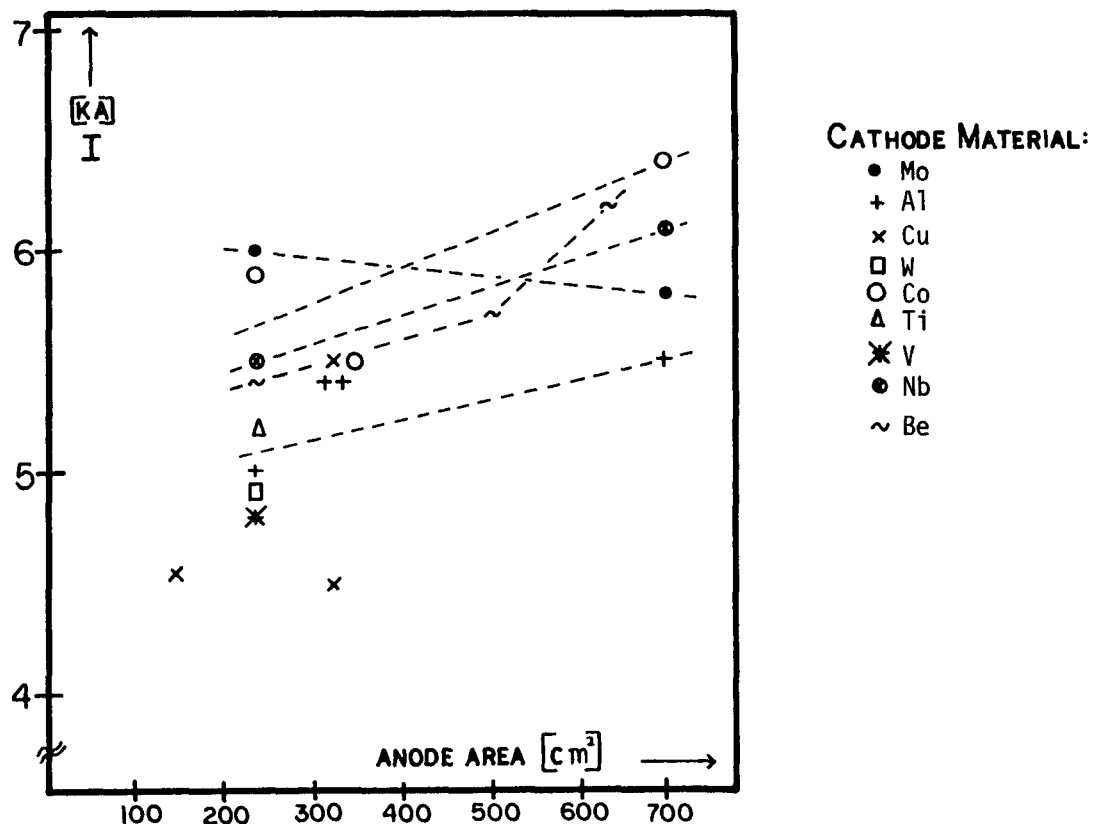


Figure 27. Interruption Ability as Function of Anode Area with 15  $\mu\text{f}$  of Parallel Capacitance.

Table II

MAXIMUM INTERRUPTION ABILITY FOR VARIOUS CATHODE MATERIALS  
WITH 0.35 TESLA MAGNETIC FIELD APPLIED. PARALLEL CAPACITANCE 15  $\mu$ F.

Anode Area cm <sup>2</sup>	690	620	500	320	230
Cathode Material and Corresponding Interruption Ability	Co-6.4 kA Nb-6.1 kA Al-5.8 kA Mo-5.8 kA	Be-6.2 kA	Be-5.7 kA	Co-5.5 kA Cu-5.5 kA Al-5.4 kA	Co-5.9 kA Nb-5.5 kA Be-5.4 kA Ti-5.2 kA W-5.1 kA V-5.8 kA

### Design Options

The coaxial electrode geometry with axial offset is an optimum arrangement with respect to switching performance. This leaves room for some variations which were tested.

Usually the trigger electrode is attached to the cathode. On the other hand, it may be desirable to separate the trigger electrode from the main cathode. For example a very bulky or a liquid metal cathode may be desired for long operating life. An arrangement is shown in Figure 28 where the separation is achieved. An auxiliary cathode with internal trigger electrode is mounted on the envelope end plate opposite from the main cathode. The auxiliary cathode and main cathode are connected through a  $10 \Omega$  resistor which limits the vacuum arc current carried by the auxiliary cathode. The commutation of the arc current from the auxiliary cathode to the main current involves a time delay of about 100  $\mu$ sec, depending upon the geometry and voltage settings. The auxiliary cathode with the internal trigger electrode is shaped like a plasma gun in order to direct a high velocity plasma stream at the main cathode. The switch-off performance is not influenced by the introduction of an auxiliary cathode.

In order to overcome the observed limit on the interruption current, a circuit modification was tried which reduces the vacuum arc current at the time of magnetic field application. A winding, series connected to the anode, was arranged in close coupling with the magnetic field coil. The magnetic field pulse induces a current into the anode lead winding which reduces the arc current. See Figure 29. It was hoped that the direct reduction of the arc current plus the action of magnetic modulation would increase the switching ability. Tests were performed with a magnetic field coil of 16 turns and an anode series coil of 13 turns. The switching ability was not improved by this arrangement. One reason is an insufficient magnitude of the counter-current induced in the anode series coil. Limited by the power supply impedance, the counter-current measured 1.4 kA peak value. (6.8 kA were induced in the short circuited anode series coil). Applying parallel capacitance produces oscillatory wave trains which do not appear useful for a fault current limiter.

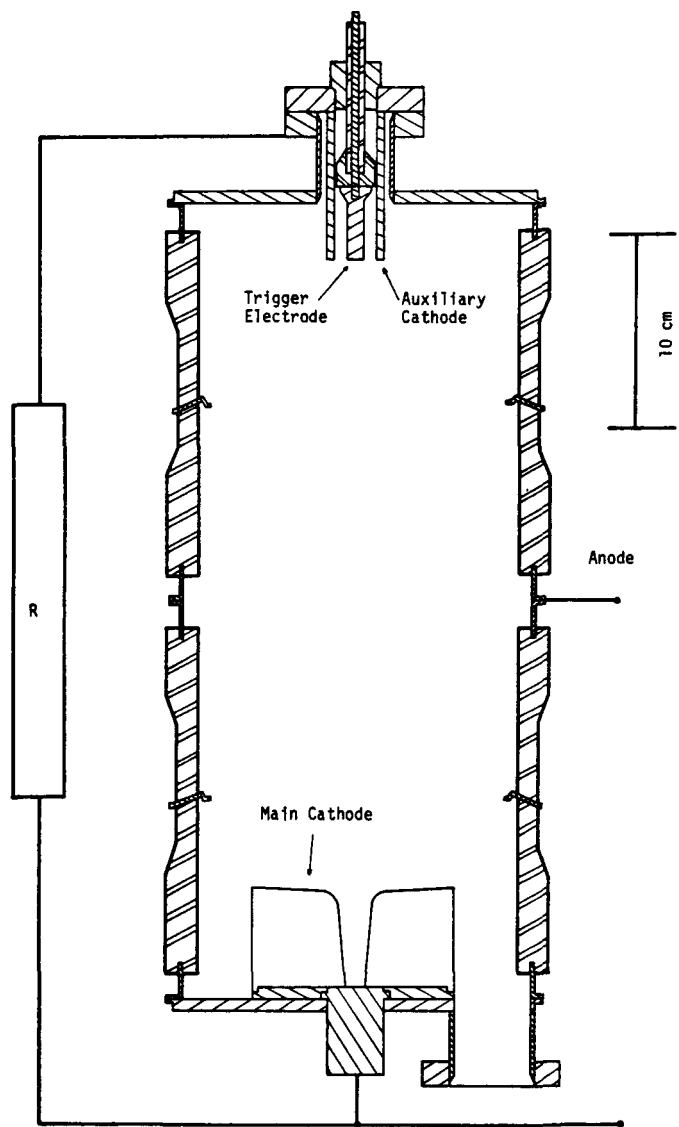


Figure 28. Alternate Trigger Arrangement with Auxiliary and Main Cathode.

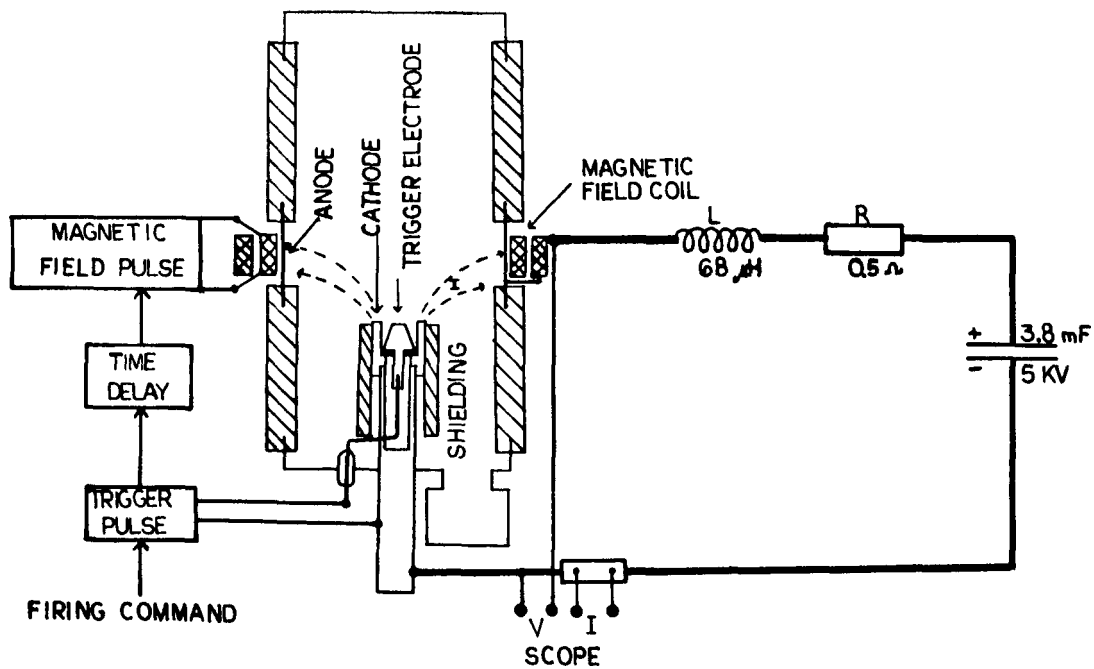


Figure 29. Alternate switching circuit using one coil in series connection to the anode, closely coupled with the pulsed magnetic field coil.

Further experiments were made with only an anode series coil connected. The anode current produces a magnetic field which leads to self-shut off or continuous current limitation, depending on the available current. Measurements were taken with a molybdenum cathode mounted 2.5" below the anode of  $690 \text{ cm}^2$  area. The self-limited current as a function of the available current is given in the following Table.

TABLE III  
CURRENT LIMITED BY AN ANODE - SERIES - COIL

<u>22 turn coil</u>		<u>13 turn coil</u>	
<u>Available Current</u>	<u>Limited Current</u>	<u>Available Current</u>	<u>Limited Current</u>
KA	KA	KA	KA
1.52	0.64	1.85	0.59 self-shut off after 54 $\mu$ sec.
2.20	1.58		
3.41	2.70	2.75	1.75
4.47	3.70	4.55	3.2

Saturable iron cores surrounding the circuit conductor are known to increase the switching performance of vacuum interrupters used with current injection for d.c. circuit interruption. The benefit is derived from a decreased fall of current  $dI/dt$  shortly before current zero.

Suitable iron cores with a flux rating of 0.04 V·sec were placed around the cable connecting to the anode. No improvement in the switching performance could be noted.

## TESTING IN THE 60 HZ LABORATORY

Testing on the capacitor bank power supply with series inductor allows efficient evaluation of the magnetically switched vacuum arc. For a demonstration of applicability to 60 Hz power systems one test series was conducted on a direct test circuit in the Greensburg Power Test Laboratory. Test power is delivered by the local utility through a 25 kV line. An oil circuit breaker on the 25 kV side serves as the making switch and backup breaker. A 5 kV or 7.5 kV tap on the transformer secondary was used. Up to 90 MVA of test power is available. See Figure 30.

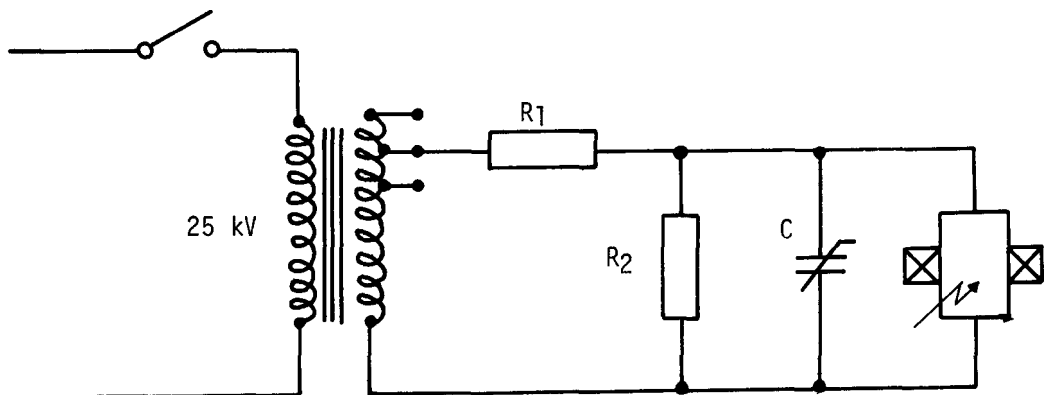


Figure 30. Diagram for Testing the Vacuum Arc Commutator on a 60 Hz Power System.

Waterbath resistors  $R_1$  and  $R_2$  determine the "limited fault current". The vacuum device is triggered on the rising portion of a current loop, shorting out resistor  $R_2$ . This constitutes "initiation of the fault". After a fraction of a millisecond the magnetic field pulse is applied to the vacuum device. In the case of successful "fault current limitation" the vacuum device ceases conduction and the current is commutated into resistor  $R_2$ , thus effecting a controlled current limitation in the circuit.

A typical test oscillogram is reproduced in Figure 31.  $t_1$  designates the time where the "fault is established" by triggering the vacuum device. At  $t_2$  the current is commutated into the fault current limiting resistor parallel to the vacuum device.  $t_2 - t_1$  is the time of conduction in the magnetically controlled vacuum device. The prospective fault current, shown as a dashed line, would have reached 6 kA. The current was limited to 4.35 kA by magnetic switching of the vacuum device at  $t_2$ .

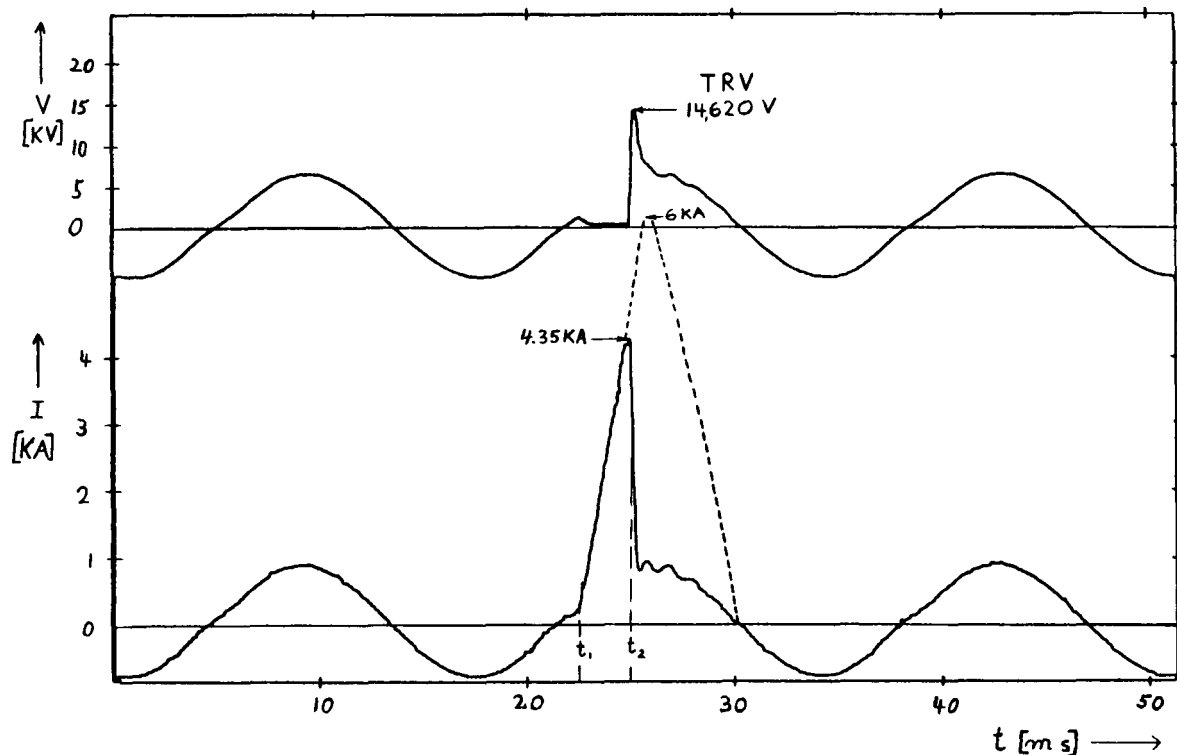


Figure 31. Typical Test Oscillogram of Fault Current Limitation in the Power Test Laboratory.

Figure 32 shows a summary of values for currents commutated and the corresponding transient recovery voltages (TRV).

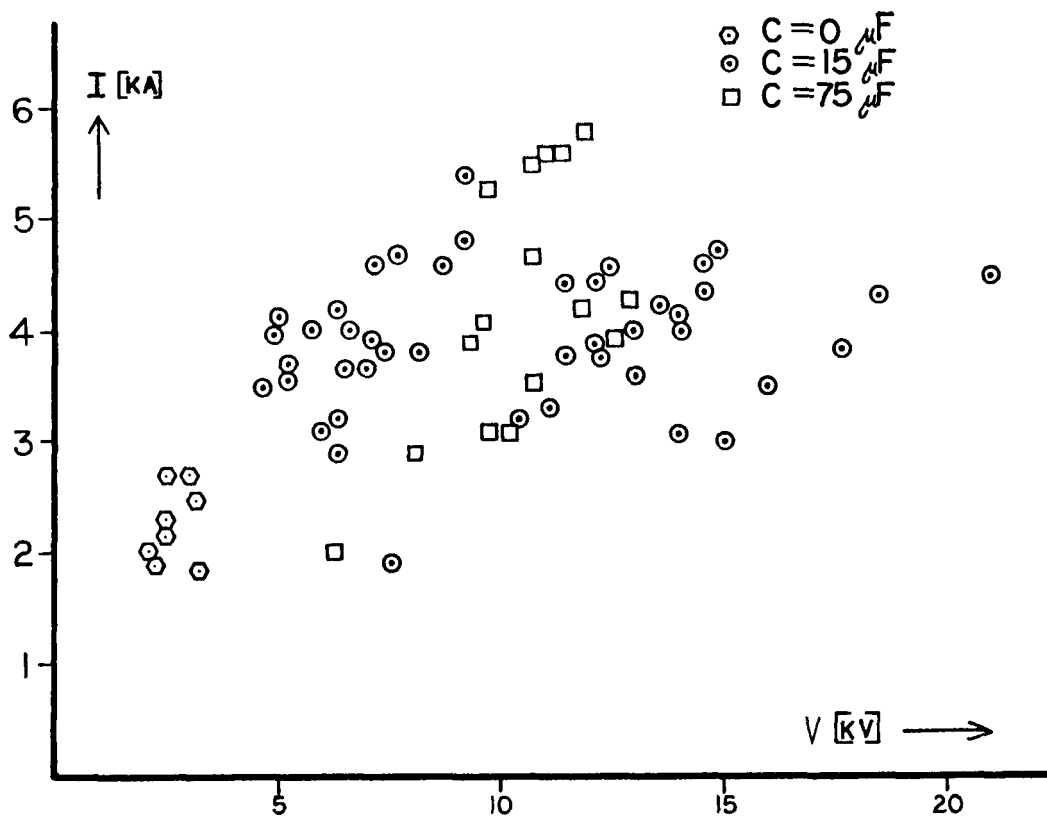


Figure 32. Commutated Current and TRV Voltages of 60 Hz Power Lab Tests.

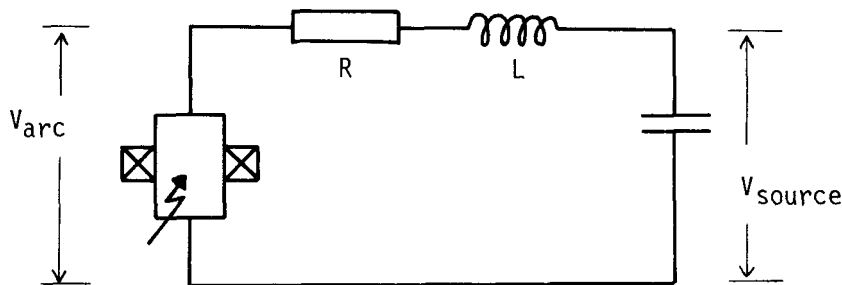
Over 250 test shots were performed with one vacuum assembly using a cobalt cathode, an anode of  $690 \text{ cm}^2$  area and a peak magnetic field of 0.82 Tesla. Triggering was reliable. The test series was terminated when the vacuum envelope failed due to a poor terminal connection external to the vacuum which caused accidental arcing. The vacuum device performed reliably within its area of capability.

## THEORY OF COMMUTATION

The vacuum commutator changes state upon command by application of the magnetic field pulse. Two modes of operation have been observed, depending upon the amount of capacitance parallel to the vacuum device.

### A. No parallel capacitance

The standard theory of D.C. switching in an inductive circuit applies. The summation of voltage terms in the test circuit yields:



$$V_{\text{source}} = L \frac{di}{dt} + iR + V_{\text{arc}}$$

or

$$L \frac{di}{dt} = V_{\text{source}} - (V_{\text{arc}} + iR)$$

DC circuit interruption at positive current  $i$  is indicated by a negative  $L \frac{di}{dt}$  term. This requires that the arc voltage and resistive voltage drop  $dt$

exceed the source voltage. In particular near current zero, where the resistive voltage drop vanishes, a high arc voltage is required. At a few amperes of current the arc voltage rises abruptly to the recovery voltage, because the cathode spots cease emission below the current chopping level.

The implication of this consideration is that switching without parallel capacitance will be limited to relatively low source voltages that can be exceeded by the attainable arc voltage.

An example of a switching operation without parallel capacitance is shown in Figure 33. The magnetic field pulse is applied at the 0.5 msec time mark. The current decreases linearly from 3.2 kA until the 0.64 msec time mark where the circuit is interrupted. The voltage terms of the previous equation are drawn over the actual voltage trace.

$$L \frac{di}{dt} = 66 \cdot 10^{-6} \frac{3 \cdot 2 \cdot 10^3}{1 \cdot 4 \cdot 10^{-4}} = 1.5 \text{ kV}$$

$$i R = 3 \cdot 2 \cdot 10^3 \cdot 0.55 = 1.8 \text{ kV}$$

The source voltage corresponds closely to the charge remaining on the storage capacitor bank after circuit interruption. Given some uncertainty in the circuit parameters, the agreement between the measured and calculated voltage trace is reasonable.

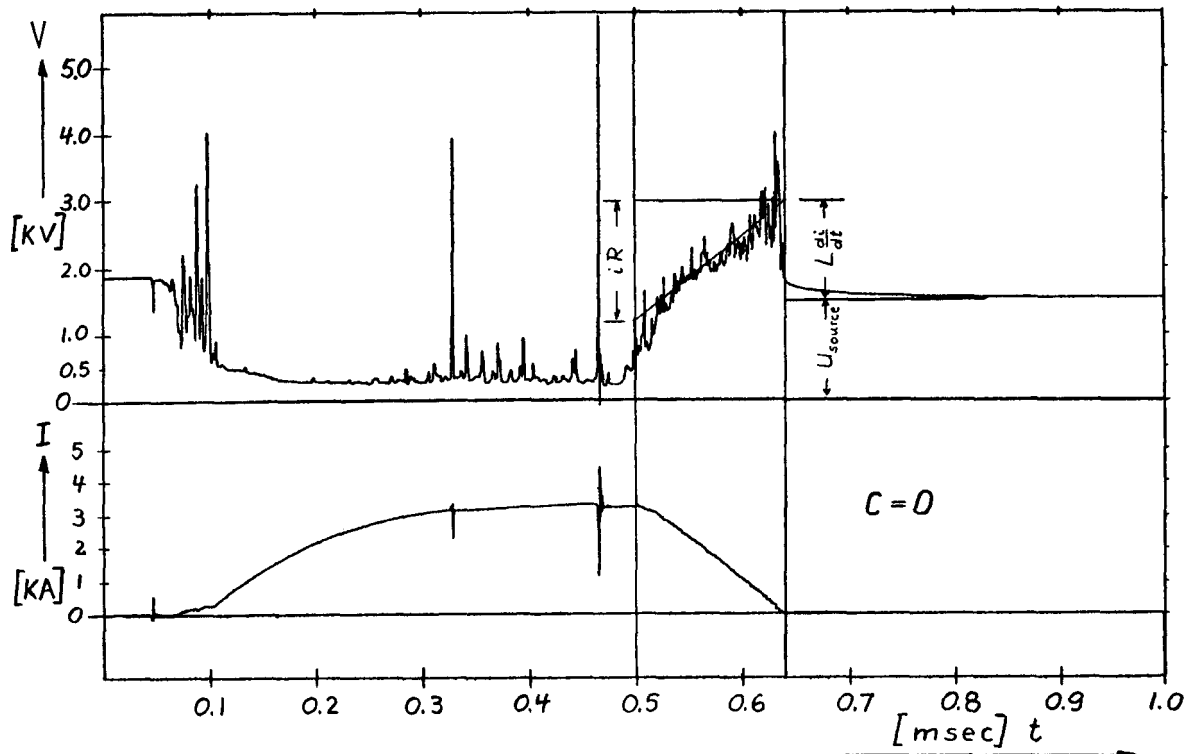
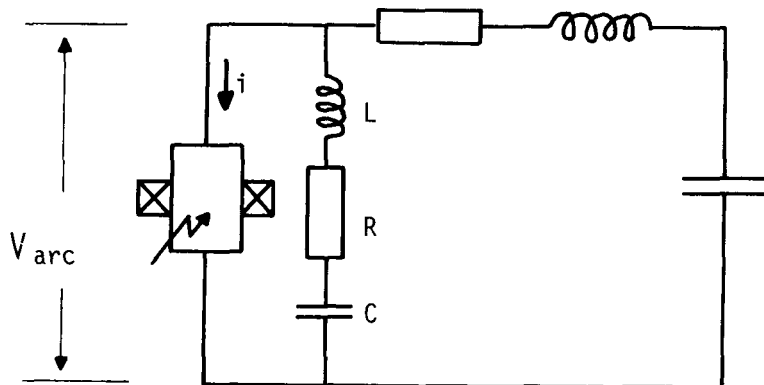


Figure 33. Vacuum Arc switched off by Magnetic Field of 0.62 Tesla Peak Magnitude. Anode area  $320 \text{ cm}^2$ . Aluminum Cathode.

B. Capacitor Parallel to the Vacuum Commutator.

A capacitor placed in parallel with the vacuum commutator involves by necessity circuit inductance and resistance as part of the loop.



The summation of voltage terms yields:

$$L \frac{di}{dt} + R \cdot i + \frac{1}{C} \int i \, dt + V_{arc} = 0$$

$$L \frac{d^2i}{dt^2} + R \frac{di}{dt} + \frac{i}{C} + \frac{d V_{arc}}{dt} = 0$$

$$\text{with } \frac{d V_{arc}}{dt} = \frac{d V_{arc}}{di} \cdot \frac{di}{dt}$$

$$L \frac{d^2i}{dt^2} + \left( R + \frac{d V_{arc}}{di} \right) \frac{di}{dt} + \frac{i}{C} = 0$$

This is the differential equation for an RLC oscillator with the arc characteristics included. The well-known solution for harmonic oscillations results if

$$\left( R + \frac{d V_{arc}}{di} \right)^2 < 4 \frac{L}{C}$$

Amplification occurs for:

$$\frac{d V_{arc}}{di} < R$$

The term  $\frac{d V_{arc}}{di}$  refers to the voltage current characteristic of the vacuum arc.

A negative characteristic can be expressed as a negative resistance. The last criterion states that self-sustaining oscillations can be excited if the combined resistance of arc and circuit is negative. The frequency of these oscillations will be:

$$f = \frac{1}{2\pi \sqrt{LC}}$$

We know from measurements that the vacuum arc voltage vs. current characteristic becomes strongly negative when the magnetic field is applied. Oscillations in arc current and voltage do appear when the magnetic field is applied.

See Figure 34.

The frequency of these oscillations varies with the amount of parallel capacitance as expected. Circuit interruption can occur when the vacuum arc current crosses the zero line. The interruption performance will depend upon the current magnitude; the  $\frac{di}{dt}$  and  $\frac{dv}{dt}$  near current zero, cathode material and design. (Actual values observed with  $3.8 \mu F$  of parallel capacitance are  $0.7 kA$  and  $0.66 kV$   $\mu sec$ ).

From vacuum interrupters it is known that  $\frac{di}{dt} = 1.0 kA/\mu sec$  and  $\frac{dv}{dt} = 20 kV/\mu sec$  are attainable.

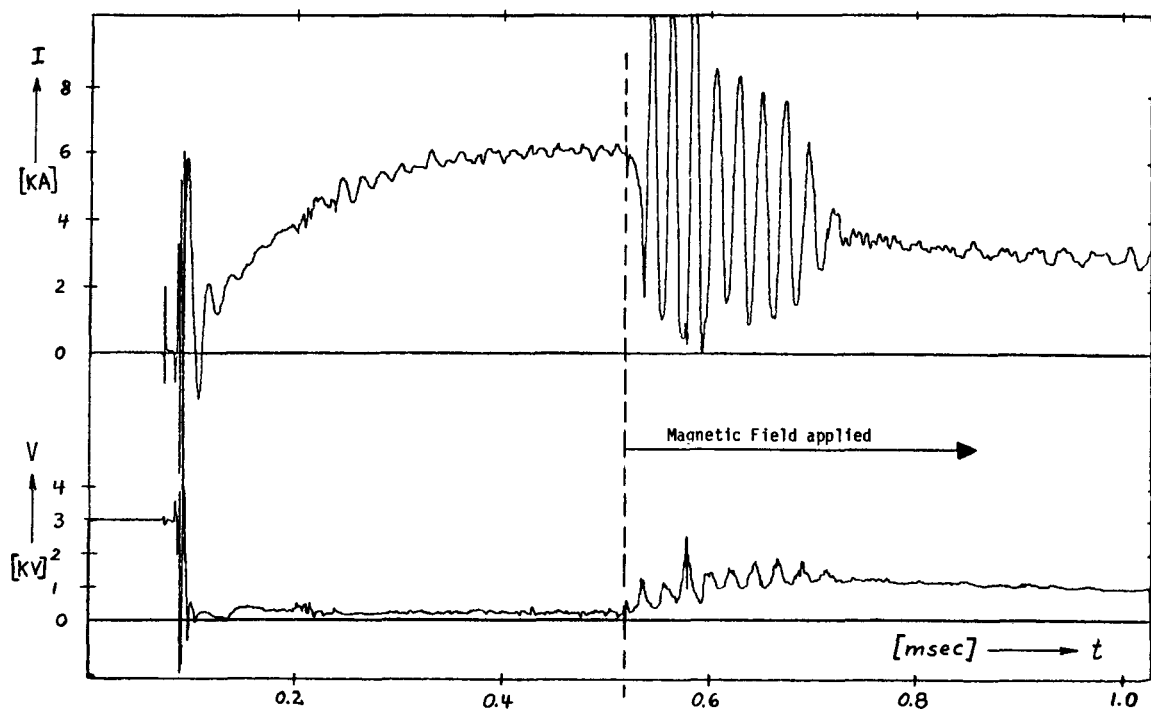


Figure 34. Unsuccessful Vacuum Arc Switch Off with Parallel Capacitor ( $C = 15 \mu F$ ). Peak Magnetic Field .72 Tesla. Anode Area  $690 \text{ m}^2$ . Niobium Cathode.

### Section 3

#### DISCUSSION

##### VACUUM ARC PHYSICS

Vacuum arcs with plane-parallel electrodes and also coaxial geometries are reviewed in Appendix A. Applicable literature references are summarized in Appendix C.

In the experiments with coaxial electrodes we observe uncommonly high values of arc voltage in the kV range. This needs an explanation. We need to analyze the location and the source of the voltage drop.

The floating potential measurements (See Figure 14) show that the voltage drop occurs in front of the anode. This observation agrees with more elaborate studies performed on the Penning discharge. Our geometry is similar to the Penning discharge device as investigated by Knauer. (See Appendix C) One difference is that the Penning discharge employs a cold cathode and a low pressure gas filling which does not lead to the high speed cathode jets that are so important in the operation of a vacuum arc device. Knauer gives a detailed description of the sheath which forms in a magnetized plasma in front of the anode. Electric field strength in the order of 8 kV/cm is measured within a narrow anode sheath, while the center of the discharge remains near cathode potential. Several papers, reviewed in Appendix C, provide the theory for Knauer's observations. Values of current density and electron density differ appreciably. But it appears that the theories of Appendix C also apply to the magnetically modulated vacuum arc. Table IV compares values of current and electron density for vacuum arcs and Penning discharges.

The average electron density, as determined by microwaves in the present study, lies between the value for a vacuum arc with plane-parallel electrodes and the one reported for Penning discharges. The microwaves are not able to show a local reduction of electron density because the measurement is averaged over the diameter of the discharge device.

TABLE IV  
COMPARISON OF CURRENT DENSITY AND ELECTRON DENSITY  
IN FRONT OF THE ANODE

	Vacuum Arc Between Plane-Parallel Electrodes Boxman (4).	Magnetically Modulated Vacuum Arc	Penning Discharge Knauer (2), (3).
Current Density A/cm <sup>2</sup>	152	~10	$7 \cdot 10^{-5}$
Electron Density cm <sup>-3</sup>	$5 \cdot 10^{14}$	$\sim 10^{12}$ Averaged as Measured by Microwaves	$2 \cdot 10^{10}$
Comment	Copper-Electrodes 25 mm diameter 9 mm gap 3 kA Arc, B=0	See Fig. 14 typically 6 kA arc $B \sim 150$ mT	$2 \cdot 10^{-4}$ Torr of Hydrogen Anode diameter 1.6 cm $B \sim 150$ mT
Discharge Voltage	~ 40 V	~ 2 kV	~ 2 kV

High plasma density (equivalent to electron density) in front of the anode is essential for current conduction at low arc voltage. The cathode emits most of its erosion products in the form of a high velocity plasma stream rectangular to the cathode surface. In the case of plane-parallel electrodes the plasma jet impinges on the anode, leading to high values of plasma density and correspondingly low arc voltage.

The present coaxial geometry of the magnetically modulated vacuum arc is such that the cathode jets do not directly reach the anode. It is postulated that the plasma in front of the anode becomes too tenuous to maintain charge neutrality. A space charge layer forms which requires a large potential drop in order to provide continuity for the arc current. The high impedance mode can exist without applied magnetic field, depending on discharge geometry, cathode material, current magnitude, trigger energy, etc. It is observed that the arc voltage rises steeply if a critical value of anode current density is

exceeded. The high impedance mode is most pronounced for cathode materials with low atomic weight and high melting point. High arc voltages are associated with high frequency relaxation oscillations in the range of 40 KHz. One may assume that these arc voltage fluctuations relate to oscillations in the density and width of the electron space charge layer.

The existence of the high impedance mode without applied magnetic field is somewhat spontaneous. Applying the magnetic field creates the high impedance mode with certainty. One may think of the magnetic field modulating the plasma density near the anode which in turn creates the plasma sheath. Magnetic focusing of the cathode jet would reduce the plasma density in front of the anode (See Appendix A). A plasma sheath usually assumes the width of about 10 times the Debye Length. The voltage-current relation of a space charge layer can be calculated from the Child-Langmuir relation (5). The observed anode current density and potential drop indicate a space charge layer of a few mm thickness. This is in a reasonable relation to the Debye Length as calculated from plasma parameters known from the literature.

The present measurements show that the magnetic field strength determines the magnitude, but not the frequency of the oscillations during the magnetic modulation. This observation rules out a rotating current spoke as the source of oscillation. The frequency of a rotating instability would grow with the magnetic field strength.

#### FEASIBILITY OF APPLICATION

We are concerned with the feasibility of a practical device and its application in a fault current limiter system. The present study has shown that a switching device based on magnetic modulation of arc voltages can be built with materials and processes that are common in the manufacture of vacuum interrupters. The choice of cathode material is not critical. Beryllium is not justified because the toxicity is not sufficiently balanced by superior interruption ability. Copper, cobalt and the refractory metals are a more practical choice.

The anode's capacity for heat absorption is no problem if the switching time is on the order of a millisecond (6). Reliable triggering of the vacuum arc is attainable with proper design.

The present design using a magnetic field coil outside the vacuum envelope leads to a relatively slow rise of the magnetic field strength. Nevertheless, current switch-off with a rate of fall of current between 100 and 200A/ $\mu$ sec has been attained. 5 to 6.5 kA of current can be interrupted reliably with about 15 $\mu$ F of capacitance parallel to the vacuum device. Higher currents may be possible with an anode diameter over 19 cm (7.5"). Testing was conducted with available transient recovery voltages (TRV) up to 20 kV. With this value the limit of capability of the device was not reached.

The objectives for a vacuum arc commutator require 9 kA of interruption current and 60 kV transient recovery voltage. It appears that the interruption requirement can be met with larger anode diameter and increased parallel capacitance. 60 kV of TRV may require two vacuum devices in series. The feasibility of a vacuum arc commutator appears promising as a device. But the same cannot be said for its application in an AC fault current limiter system. The switching device is polarity sensitive, requiring two units back to back for AC applications. Further, use of the triggered vacuum arc commutator still requires the development of a fast acting mechanical by-pass switch. The resistive fault current limiter system with triggered vacuum arc commutator appear too complex for being practical.

DC applications would be more suitable for the magnetically modulated vacuum arc. Amplification in the MW power range has been demonstrated by the current project. Gilmour's earlier work demonstrated switching operations with KHz repetition rates (1). A compact, permanently sealed switching tube can be built which may find applications in airborne power conversion equipment, switching for inductive energy storage, pulse generators, etc. Competing technology is either lower in interruption ability or more complex. A magnetically controlled switch which is based on hydrogen thyratron technology has attained 600 A interruption at 20 kV (7). The Crossed Field Tube of Hughes Research Labs. has attained 10 kA interruption at 100 kV for large size tubes with 8,000 cm<sup>2</sup> of electrode area. This tube cannot be sealed permanently because a control system is needed to keep the internal helium pressure constant (8).

#### RECOMMENDATION FOR FURTHER PURSUIT

Fast acting DC switching devices are required in a multitude of power-conditioning and protection applications. The results attained under this project should be reviewed with respect to upcoming applications. An operational device has been demonstrated under realistic hardware conditions. Further extension of the current and voltage level together with high repetition rates appears feasible.

## REFERENCES

1. A. S. Gilmour, D. L. Lockwood. The Interruption of Vacuum Arcs at High DC Voltages. IEEE Trans. on Electron Devices Vol. ED-22 No. 4, pp. 173-180 (April 1975).
2. W. Knauer. Mechanism of the Penning Discharge at Low Pressure. Journ. Appl. Phys. Vol. 33, No. 6, pp. 2093-2099 (June 1962)
3. W. Knauer and M. A. Lutz. Measurement of the Radial Field Distribution in a Penning Discharge by Means of the Stark Effect. Appl. Physics Letters, Vol. 2, No. 6, pp. 109-111 (March 1963)
4. R. L. Boxman. Magnetic Constriction Effects in High Current Vacuum Arcs Prior to the Release of Anode Vapor. Journ. Appl. Phys. Vol. 48, No. 6, pp. 2338-2344 (1977)
5. J. D. Cobine. Gaseous Conductors. pp. 125 Dover Publications 1958.
6. C. D. Bowman, et al. Analysis of a Vacuum Arc Fault Current Limiter for Use in Power Systems. Paper, 1979 IEEE Winter Power Meeting New York, New York
7. R. F. Caristi et al. Advances in the Development of a Gas Discharge Switch having a Repetitive Current Interrupting Capability. IEEE Conference Records of the 13th Pulse Power Modulator Symposium, pp. 227-234, Buffalo, 1978.
8. R. J. Harvey, et al. Current Interruption at Powers up to 1 GW with Crossed-Field Tubes. IEEE Trans. Plasma Science Vol. PS-6 No. 3, pp. 248-255, (1978)

## APPENDIX A

### BACKGROUND OF THE MAGNETICALLY MODULATED VACUUM ARC

The vacuum arc has been investigated extensively with regard to applications in vacuum interrupters. For a review see Ref. 3 and 4.

The term vacuum arc is used for the electric discharge conducted through ionized metal vapor in a vacuum ambient. The metal vapor is supplied from the electrodes, particularly the cathode, in the form of erosion products generated by the concentrated energy input from the arc attachment areas. It is possible to operate the anode free of erosion. Cathode erosion on the other hand is necessary as a supply of charge carriers for the discharge. This is enforced by a strong constriction of the vacuum arc at the cathode attachment area. The current density within the cathode spot reaches values of  $10^7$  A/cm<sup>2</sup>. Vapor jets are emitted from the cathode spot which extend into the vacuum at velocities up to  $10^5$  m/s. This phenomenon has been investigated and optimized for miniature electric rocket thrusters to be used for satellite control (5), (6).

It is known that these erosion products consist of high velocity electrons, ions and neutral molecules which are expelled in the general form of a cone extending at right angle from the cathode spot area.

The requirements for vacuum arcs in switchgear and electric rockets are different. Correspondingly, complementary experience has been gained by the study of vacuum arcs for both of these applications.

The electrodes of vacuum switchgear usually oppose each other. The cathode vapor jets impinge on the anode and the intervening space is filled with highly conducting plasma which conducts the current at a low arc voltage of less than 40 volts as long as the arc remains in the diffuse mode, (see Figure 1a). The existence of the diffuse mode requires a sufficient plasma density in front of the anode. Mitchell has analyzed the current carrying ability of the diffuse vacuum arc between plane parallel electrodes (7). He defines a critical

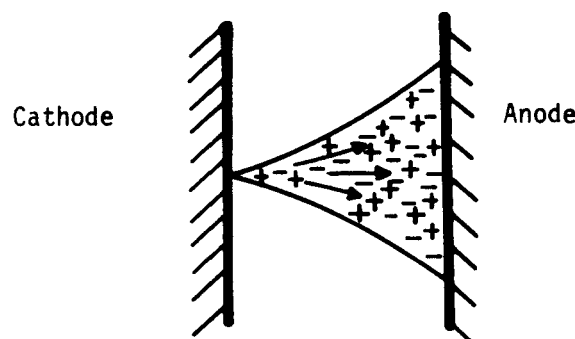


Figure 1a

Plane - Parallel Geometry  
Low Arc Voltage

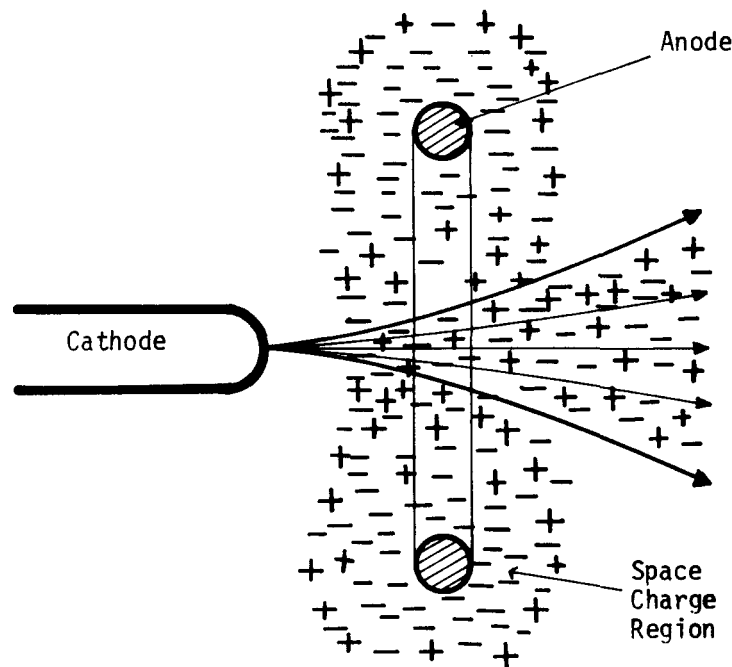


Figure 1b

Ring Anode Outside of  
Cathode Plasma Jet.  
High Arc Voltage Possible

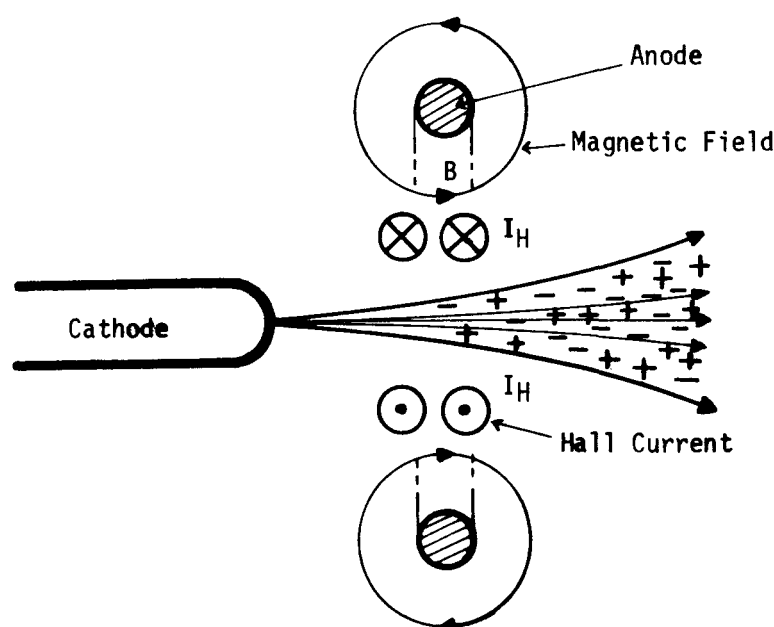


Figure 1c

Ring Anode Outside of  
Cathode Plasma Jet,  
With Magnetic Field and  
Hall Current,

Impedance Modulation and  
Switching Possible.

"starvation current density" above which the vacuum arc transforms from the diffuse to the constricted mode which leads to anode melting for high current arcs.

The electrode arrangement of the present investigation is derived from electric thrusters, where a coaxial anode surrounds the cathode in such a way that the cathode vapor jets exhaust unimpeded into vacuum (Figure 1b). The plasma density at the anode will be rather low. Charge separation will occur and the electron space charge can build up very high values of arc voltage. A space charge field can attain very high values in the order of  $10^5$  volts. High voltages can only exist in an area of low particle density because otherwise electron collisions with neutrals would create ionization breakdown.

Arc voltages exceeding a few hundred volts have not been observed in plane parallel geometries of Figure 1a. This must be due to the relatively high density of neutrals in front of the anode.

In Figure 1b, on the other hand, the anode is arranged outside of the plasma cone extending from the cathode. High electric fields can therefore exist in the anode area up to a time where heating of the anode leads to desorption of gases or evaporation of metal vapor. One can expect that the performance of the device will depend upon the cleanliness and surface properties of the anode.

Gilmour observed that a very effective impedance control of the vacuum arc could be achieved by the application of magnetic fields to a coaxial electrode geometry. The crossing of electric and magnetic field lines results in the generation of an annular Hall current flowing in the inter-electrode space. The magnetic field in Figure 1c is generated by a ring current flowing in the annular anode. The existence of a Hall current increases the impedance between cathode and anode. This effect is generally known and can be predicted from basic equations of electric conduction in plasmas with magnetic fields applied, for example, see Ref. 5. This effect may be contributing, but it cannot explain the observed magnitude of magnetic modulation.

The coaxial geometry as shown in Figure 1c is a preferred geometry for generating an annular Hall current without the use of additional electrodes. Theory also requires that the discharge uniformly fills the inter-electrode space. A constricted arc column would develop a Hall-voltage perpendicular to the arc column and would start rotating. No evidence for a rotating current spoke has

been observed. An annular Hall current generates a pressure gradient which is directed radially inward. In this manner the magnetic field is able to control the diameter of the cathode vapor jet and thereby to control the plasma density in front of the anode which is related to the voltage drop in front of the anode.

#### REFERENCES

1. A. S. Gilmour Jr., and D. L. Lockwood. The Interruption of Vacuum Arcs at High dc Voltages. IEEE Trans. on Electron Devices. Vol. ED-22 No. 4, pp. 173-180, April 1975.
2. U.S. Patent No. 3,696,264, 1972. Magnetically Modulated Vacuum Arc Diode.
3. G. A. Farrall. Vacuum Arcs and Switching. Proc. IEEE Vol. 61 No. 8, pp. 1113-1136, August, 1973.
4. M. P. Reece. The Vacuum Switch. Proc. IEEE Vol. 110, No. 4, pp. 793-811, April, 1963.
5. A. S. Gilmour and D. L. Lockwood. Pulsed Metallic - Plasma Generators. Proc. IEEE Vol. 60, No. 8, pp. 977-991, August, 1972.
6. R. Dethlefsen. Performance Measurements on a Pulsed Vacuum Arc Thruster. AIAA Journal Vol. 6, No. 6, pp. 1197-1199, June, 1968.
7. G. R. Mitchell. High Current Vacuum Arcs. Proc. IEEE Vol. 117, No. 12, pp. 2315-2332, December, 1970.

## APPENDIX B

### TRIGGER OPTIONS

Upon command a Fault Current Limiter must rapidly separate mechanical contact and insert additional impedance into the circuit.

Current must be commutated into the vacuum arc switching element for subsequent transfer into the current limiting impedance.

The existence of a vacuum arc is assured if mechanical contacts are separated under vacuum. This is certainly the simplest method of starting the vacuum arc. The disadvantage is a severe limitation in choosing optimum geometries for the purpose of attaining high values of arc voltage and proper switching in the vacuum arc.

As a goal under the present project, it was therefore decided to work with triggered vacuum arc discharges. A fast acting mechanical by-pass switch can generate 500 V arc voltage. 500 V is therefore the level where successful triggering must be attained.

The dielectric strength of a vacuum gap is exceedingly high. Injecting electric charge carriers will cause rapid breakdown because of the high mobility in vacuum.

The trigger charge carriers are usually generated by applying a voltage such that a small discharge results.

The most effective one out of several possible combinations is a positive trigger pulse applied to a trigger electrode which is attached to the cathode. The trigger discharge establishes cathode spots on the main cathode which provide charge carriers for the trigger and the main discharge.

Various trigger arrangements have been developed for use in ignitrons, triggered vacuum gaps and small electric rocket thrusters used for satellite control. These differ basically in the phenomenon used for creating the initial charge carriers for the trigger discharge. Five alternatives are discussed below. Illustrations are shown in Figure 1.

#### Laser Pulse

A short, high power pulse from a laser can be admitted to the vacuum area through a window. A pulse of sufficient magnitude impinging on the cathode can release sufficient plasma for triggering with a delay time of a few micro-seconds. The disadvantage of this scheme is high cost and metal vapor coating on the optical window. See Figure 1a.

#### Field Emission

Field emission of electrons from a narrow gap of about 0.1 mm between a trigger electrode and the cathode has been used in pulsed X-ray tubes for many years. (1). A trigger pulse of 20 to 30 kV is sufficient to cause breakdown of the main gap. See Figure 1b.

#### Exploding Metal Film

Vacuum breakdown across insulator surfaces coated with thin metallic or semiconducting layers can be attained with rather low voltages on the order of 200 V. The geometry must be such that the resulting vacuum arc will repeatedly deposit a metal layer on the insulator surface extending between the trigger and the main electrode. (See Figure 1c) This method has previously been used for triggering vacuum arc satellite control thrusters (2), (3). A lifetime of more than  $10^6$  discharges has been demonstrated for low energy discharges. A problem of uneven and excessive insulator erosion exists at current levels of several kA. This is particularly severe for refractory cathode materials. Hard insulators on the other hand, such as high density alumina, boron carbide and diamond show the lowest erosion rates. (2).

The physics of triggering vacuum arcs by discharges across insulating surfaces for various polarity combinations is described in Ref. 4.

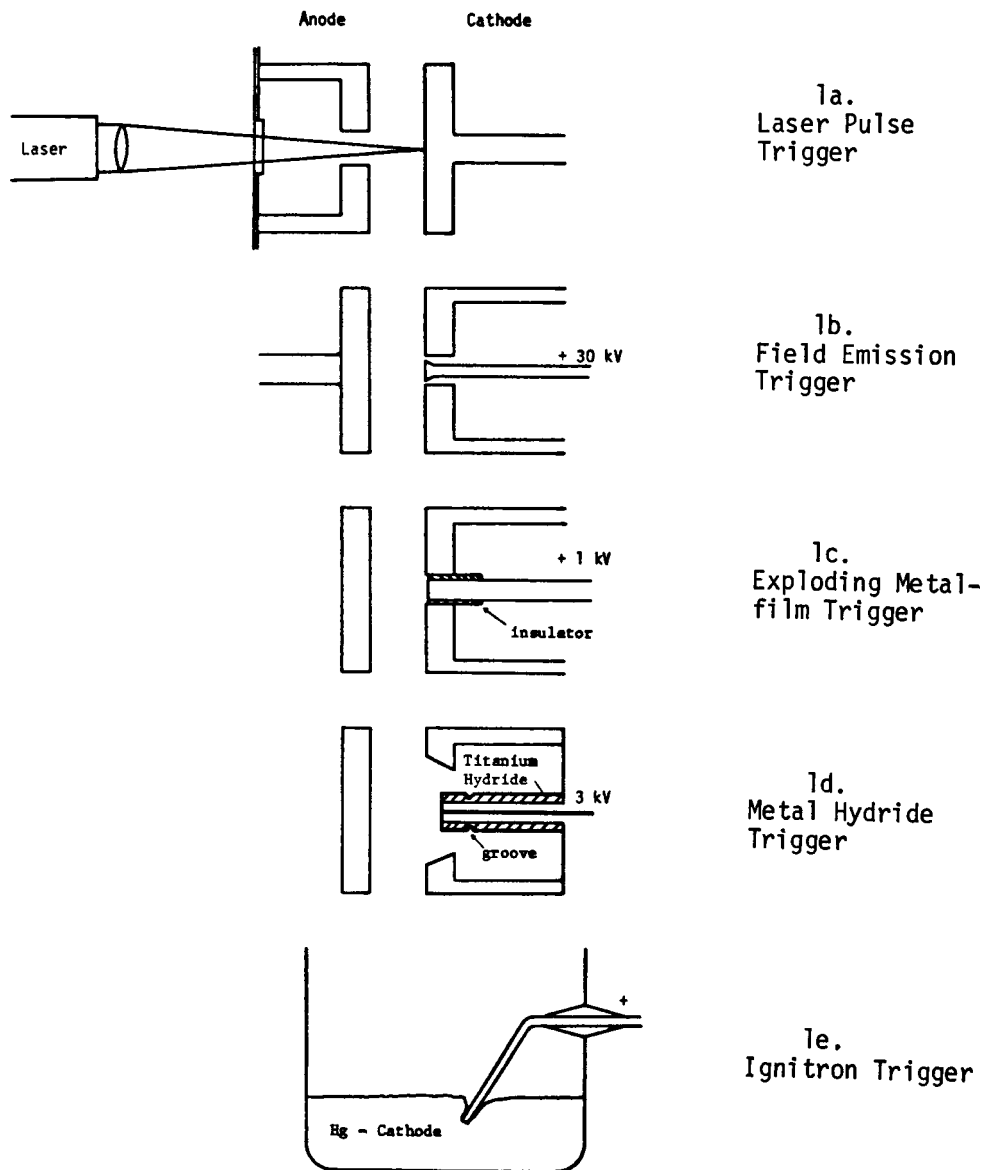


Figure 1. TRIGGER OPTIONS.

A positive pulse applied to a trigger electrode attached to the cathode leads to the establishment of a cathode spot on the main cathode which supplies current to the trigger and also to the main current. The initial cathode spot will split and multiply as required by the main current. It is shown that the need for cathode spot multiplication limits the rate of rise of current to a value of  $dI/dt < 10^7$  A/sec.

Generally a stronger trigger discharge is required if the trigger electrode is attached to the anode. The plasma emitted into the main electrode gap will not support a high electric field in its bulk, forcing all the voltage drop across a positive sheath which forms in front of the cathode. The resulting cathode electric field strength reaches very high values leading to breakdown between the conducting plasma and the cathode.

Further experiments on triggering across insulating surfaces are reported in Refs. 5 and 6. The time delay between trigger pulse and main discharge can be as low as 0.1  $\mu$ sec if the trigger energy is sufficient and the main gap voltage in the kV range. This is independent of the tested insulator materials. (Alumina, steatite, barium titanite, silicon carbide and boron nitride.) Only about 500 useful shots were obtained from each device. The end of useful life was determined by either excessive erosion of, or metal deposition, on the trigger insulator surface. Reportedly barium titanite is particularly difficult to coat with metallic layers, leading to an open trigger circuit after repeated firing. Boron nitride on the other hand is easiest to coat. This can lead to decreasing resistance between the trigger electrode and the main electrode. The minimum trigger voltage is found to be 300 V. Of course, all these findings depend upon the electric circuits and the device geometry.

Ref. 7 reports the results of a similar vacuum trigger study with a main gap of 1 mm and a main voltage of 220 V. The trigger gap across an insulating surface is 0.1 mm wide. It is pointed out that out of a wide variety of insulator materials silicon carbide shows the lowest consistent trigger voltage below 200 V. Initial conditioning with higher voltage is needed. Trigger currents above 20 A reportedly lead to surface cracking of the insulator.

### Metal Hydride

A class of commercially available triggered vacuum gaps is based upon the use of metal hydride triggers (8). The trigger arc is initiated between two hydrogen loaded titanium electrodes separated by a small fraction of a millimeter.

See Figure 1d. The trigger electrodes are formed by cutting a circumferential groove into a titanium covered alumina cylinder. Titanium hydride is formed by heating the structure in hydrogen. The trigger assembly is mounted within the main cathode. In addition to titanium, other hydride forming metals can be used, such as hafnium, palladium, thorium, uranium, yttrium, zirconium.

The trigger delay is in the order of a microsecond with trigger voltages between 100 V and some kV and a pulse energy of about 0.01 joule. The trigger discharge releases minute amounts of hydrogen which are readily gettered by the main discharge such that the pressure within a sealed vacuum envelope is not measurably affected. Ref. 4 reports that the energy required for a hydride trigger is 10% of that required for a comparable trigger without hydride loading.

The hydride trigger has also been designed in the form of a small coaxial plasma gun which magnetically propels a high velocity plasma burst into the gap between the main electrodes. A trigger life of several thousand shots has been demonstrated.

### Ignitron Trigger

Ignitrons with a liquid mercury cathode have been used for a long time. Triggering is provided by a carbide rod which is dipped into the mercury. A depression in the mercury surface is made because mercury tends not to wet carbides. The resistance of this junction is about 200 ohm. A positive pulse of 1 to 3 kV applied to the carbide rod will establish cathode spots on the mercury surface. These provide charge carriers for breakdown of the cathode-anode gap. See Figure 1e.

## REFERENCES

1. E. Fuenfer. Dielectric Breakdown in Vacuum of Pulsed X-Ray Tubes. Zeitschrift f. Angew. Phys. H.11. pp. 426-440 (1953).
2. A. S. Gilmour, D. L. Lockwood. Pulsed Metallic - Plasma Generators. Proceedings of the IEEE. No. 8, pp. 971-991 (1972).
3. R. Dethlefsen. Performance Measurements on a Pulsed Vacuum Arc Thrustor. AIAA Journ. Vol. 6, No. 6 pp. 1197-1199 (1968).
4. R. L. Boxman. Triggering Mechanisms in Triggered Vacuum Gaps. IEEE Trans. on Electron Devices Vol. ED No. 2 pp. 122-128 (1977).
5. G. R. Govinda Raju et al. Breakdown Mechanisms and Electrical Properties of Triggered Vacuum Gaps. Journ. Appl. Phys. Vol. 47, No. 4 pp. 1310-1317 (1976).
6. G. R. Govinda Raju et. al. Firing Characteristics of a Triggered Vacuum Gap Employing a Dielectric Coated with a Semiconducting Layer. Journ. Appl. Phys. Vol. 48. No. 3 pp. 1101-1105 (1977).
7. N. Vidyardni and R.S.N. Rau. A Simple Triggered Vacuum Gap. Journ. Phys. E., Scient. Instrum. Vol. 6 pp. 33-34, G.B. (1973).
8. J. M. Lafferty. Triggered Vacuum Gaps. Proceedings of the IEEE Vol. 54, No. 1, pp. 23-32 (1966).

## APPENDIX C

### LITERATURE SURVEY

- E. Inall et al.  
Application of the Hall Effect to the Switching of Inductive Circuits.  
Rev. Sci. Instrum. Vol. 48. No. 4, pp. 462-463 (April 1977).  
  
A pulsed magnetic field is applied to a current carrying disk of indium antimonide semiconductor material. The crossing of electric and magnetic field lines leads to an effective resistance increase due to the Hall effect. The application of 6 Tesla magnetic field strength leads to a resistance increase by two orders of magnitude. The geometry and mode of operation of the semiconductor device is similar to the magnetically modulated vacuum arc. The semiconductor employs a solid state plasma while the vacuum arc works with a gaseous plasma. The attained resistance modulation is comparable. The solid state device is power limited. 3 kA pulses of 160  $\mu$ sec duration lead to destruction by melting. The solid state device also does not allow dielectric recovery.
- W. Knauer  
Mechanism of the Penning Discharge at Low Pressures.  
Journ. Appl. Phys. Vol. 33 No. 6 pp. 2093-2099 (June 1962).  
  
The geometry of a Penning discharge is similar to the magnetically modulated vacuum arc. Knauer operated a Penning discharge with a variety of gases at pressures below  $10^{-4}$  Torr. He finds that most of the discharge voltage drop appears in a narrow sheath in front of the anode. The center of the discharge remains close to the cathode potential. These results agree with our measurements of floating potentials on the magnetically modulated vacuum arc.  
  
Knauer gives a qualitative description of the anode sheath development: The anode sheath is an area of intense ionization. Ions which originate there accelerate radially inward toward the cathode. They leave the sheath rapidly and contribute little to its space charge. The electrons in the sheath area tend to accelerate outward to the anode. But the applied magnetic field causes the electrons to spin and drift circumferentially. This magnetic trapping of the electrons in the sheath area leads to space charge formation which provides the electric strength necessary to drive the electrons to the anode accounting for the reduced mobility across the magnetic field lines.  
  
The anode current is proportional to the gas density because both the rate of ionization and the cross field mobility are proportional to the gas density. The charge density and sheath profile is therefore constant in the pressure range below  $10^{-4}$  Torr. The Penning discharge operates with a cold cathode. A difference exists to the vacuum arc where the cathode

spots emit high velocity jets of neutral and ionized metal vapor. We know from experience that the magnetically modulated vacuum arc only operates successfully if the anode is shielded from these high speed cathode jets. The conditions in front of the anode are very similar to the low pressure Penning discharge if mainly neutral metal vapor reaches this area.

Knauer further deduces the electron rotation speed from microwave resonance measurements and relates this to an electric field strength of 8.8 kV/cm in the anode sheath.

- W. Knauer and M. Lutz  
Measurement of the Radial Field Distribution in a Penning Discharge by Means of the Stark Effect.  
Applied Physics Letters Vol. 2 No. 6, pp. 109-111 (March 1963).

In further experimentation Knauer and Lutz measured the electric field strength inside the anode sheath by spectroscopic methods. 6.3 kV/cm were obtained in a particular example at 3 kV discharge voltage,  $2 \cdot 10^{-4}$  Torr of hydrogen pressure and 0.15 Tesla of magnetic field strength.

- Y. Popov  
Low Pressure Cold-Cathode Penning Discharge.  
Soviet Physics - Technical Physics, Vol. 12 No. 1, pp. 81-86 (July 1976).

For a Penning discharge at pressures in the  $10^{-4}$  Torr range and below, the dependence of discharge current on voltage and magnetic field, the thickness of the anode space-charge layer, the potential distribution, and the electron density are calculated. Calculations are compared with data of Knauer and Lutz, taken at  $2 \cdot 10^{-4}$  Torr.

- N. A. Kervalishvili and A. V. Zharinov  
Characteristics of a Low Pressure Discharge in a Transverse Magnetic Field.  
Soviet Physics - Technical Physics Vol. 10, No. 12, pp. 1682-1687 (June 1966).

Experiments and theory are correlated for the Penning discharge containing argon at pressures below  $10^{-3}$  Torr. The discharge is characterized by a sharply defined layer of negative space charge in front of the anode which sustains almost all the discharge voltage. The electron drift in the crossed electric and magnetic fields of the anode layer gives rise to a Hall current, which is almost independent of pressure. It is concluded that the electron transfer within the anode layer is due mainly to collision processes.

The thickness of the anode sheath is in the order of 1 cm. It grows weakly with increasing discharge voltage. The sheath becomes thinner with increasing magnetic field strength. It is pointed out that the alignment of the anode in relation to the magnetic field lines is critical. Perturbations on the anode surface propagate their effect into the anode space charge layer.

- N. A. Kervalishvili  
Instabilities of a Low-Pressure Discharge in a Transverse Magnetic Field.  
Soviet Physics - Technical Physics Vol. 13, No. 4, pp. 580-582 (Oct. 1968).

The discharge geometry described in the previous reference was investigated with respect to oscillations. Relaxation oscillations were found in the area of the high impedance discharge at pressures below  $10^{-3}$  Torr. The electron and ion currents are found to oscillate in phase thus compensating each other. The frequency is in the MHz region. Alignment between anode and the magnetic field is a very critical parameter.

- E. M. Barkhudarov et al.  
Anode Sheath Instability and High Energy Electrons in a Low Pressure Discharge in a Transverse Magnetic Field.  
Soviet Physics - Technical Physics Vol. 17, No. 9, pp. 1526-1529 (March 1973)

Further details are provided on the oscillation described in the previous reference. The anode sheath is unstable in the steady state; instability sets in where the electron density reaches a critical value, and many of the electrons are ejected along the magnetic field lines. As a result the sheath expands. Then the electron density in the sheath increases again and the process repeats itself.

- V. K. Kalashnikov and Y. V. Sanochkin  
Low Pressure Self-Maintained Discharge with Suppressed Electron Drift.  
Sov. Phys. Tech. Phys. Vol. 19 No. 12, pp. 1549-1557 (June 1975)

A detailed theoretical analysis is presented with correlation to experimental data. It is concluded that classical diffusion can describe electron conduction through the sheath.

- V. Chumenkov  
Theory of the Electric Discharge in a Strong Transverse Magnetic Field.  
Sov. Phys. Tech. Phys. Vol. 21 No. 6 pp. 710-715 (June 1976).

A complex mathematical treatment is given to the anode plasma sheath for conditions as used by Knauer in his experimentation. The steady state, one dimensional solutions yield profiles for the electron and ion densities, electron temperature and the potential distribution. Instabilities and relaxation oscillations are mentioned but not included in the analysis.

- E. Lutsenko et al.  
Investigation of Current Limitation in a Strong-Current Discharge.  
Sov. Phys. JETP, Vol. 42, No. 6 pp. 1050-1056 (1976)

A straight discharge in an axial magnetic field shows sudden, short time current limitations if a critical current density is exceeded and if inhomogeneities exist in the plasma. The gas density of  $10^{13}$  cm $^{-3}$  corresponds to the density used in the Knauer experiments. The density within the magnetically modulated vacuum arc is expected to be in a similar range. A major difference with the Lutsenko experiments is the application of a magnetic field parallel to the electric current flow.

The Lutsenko experiments appear applicable to the current limitation without applied magnetic field which has been observed in the vacuum arc.

Lutsenko reports that the critical current density for spontaneous current limitation is proportional to the gas density. A triggered current limitation can also be initiated by creating a plasma inhomogeneity where a short magnetic field pulse is applied.

Lutsenko explains the observed current limitation by the creation of a double space charge layer which occurs under conditions when the directional electron velocity in the area of reduced plasma density reaches a value equal to the thermal velocity of the plasma electrons.

During the existence of the current limiting instability the circuit current is carried by a beam of fast electrons. This is associated with the emission of X-ray and RF energy.

- N. Kervalishvili  
Electron Motion and Structure of the Anode with a Deviation from  $E \perp H$  in a Low Pressure Discharge.  
Soviet Physics-Technical Physics, Vol. 20, No. 4, pp. 512-516 (1976)

Analysis and experiments are conducted for magnetic fields which are aligned slightly out of parallel with the anode surface. It is shown that the anode sheath becomes asymmetric and that the electron mobility across the magnetic field increases.